Tampere University

Sadra Miri

THE PERFORMANCE OF OPTICAL HEART RATE MEASUREMENT IN MONITORING OF GASTROINTESTINAL SURGERY PATIENTS

Master of Science Thesis
Faculty of Medicine and Health Technology
November 2021

ABSTRACT

Sadra Miri: The Performance of Optical Heart Rate Measurement in Monitoring of Gastrointestinal Surgery Patients
Master of Science Thesis
Tampere University
Degree Program in Biomedical Sciences and Engineering, MSc (Tech)
September 2021
Examiner: Associate Professor Antti Vehkaoja and Professor Jari Viik

---

Objective: The importance of heart rate variability (HRV) for the evaluation of heart condition and autonomic nervous system (ANS) in different status has resulted in attempts for expanding the use of optical heart rate monitoring (OHR) devices. OHR technology can be utilized as wristbands to provide comfort. The working principle is based on emission and reflection of light through skin and measuring the changes in blood volume in small arteries and arterioles and generating the heart rate signal by the help of algorithms within the OHR device. The objective of this thesis was to assess the performance of optical HRV monitoring in gastrointestinal surgery patients.

Materials and Methods: Data from electrocardiogram (ECG) reference and OHR wristband was collected from 31 patients after undergoing gastrointestinal surgeries. The duration of recorded data for each subject was ranging from 24 to 72 hours and approximately 1200 hours of data was collected as a whole. The signals obtained from ECG reference and OHR wristband were compared with each other and beat-to-beat error was estimated. In the next step, HRV parameters were calculated in 5-minute length intervals and measurement error of OHR was estimated. The effects of ectopic beat removal on the result of error estimation were also evaluated.

Results and Discussion: The average mean error (ME), mean absolute error (MAE) and relative mean absolute error (MAPE) of beat-to-beat comparison of the HRV data obtained from the OHR and ECG reference were -1.34 milliseconds (ms), 10.39 ms and 1.28 %, respectively. Concerning the HRV parameters estimated by the OHR device, the accuracy was varied based on the type of HRV parameter. While the relative mean absolute errors (MAPE) of SDNN and SD_2 were 9.11% and 7.54%, for RMSSD and SD_1 MAPE values were 34.28% and 34.29%, respectively. The result of beat-to-beat error estimation approves the accuracy of OHR technology for recording HRV and it can be still improved by reducing the motion artifacts. For estimating the HRV parameters through OHR technology, the accuracy is not similar for all parameters. Some parameters such as SDNN, SD_2, DFA α_1 and DFA α_2 can be reliably estimated while for RMSSD, SD_1 and pNN50 the OHR technology should be used with caution. Finally, by evaluating the cross-correlation and Bland-Altman plots it was concluded that the results obtained with OHR technology demonstrate a high agreement and correlation with the results obtained with conventional ECG device.

Keywords: electrocardiogram, error estimation, heart rate variability, inter-beat-intervals, optical heart rate monitoring

PREFACE

My thesis from the beginning till the end was full of useful learning experiences and I would like to thank my supervisor Professor Antti Vehkaoja for giving me the opportunity to be a part of this project and for his excellent supervision and guidance during every step of the thesis.

I did my thesis as a thesis worker in Päijät-Häme Joint Authority for Health and Wellbeing, Lahti, Finland, which I also would like to thank Adjunct Professor Jyrki Kössi and Specialist in surgery Juha Rinne for giving me this great chance and also providing me with the data from gastrointestinal surgery patients.

Tampere, November 2021

Sadra Miri

CONTENT

LIST OF FIGURES

LIST OF SYMBOLS AND ABBREVIATIONS

AC	Alternating Current
AF	Atrial Fibrillation
AL	Amyloid
ANN	Artificial Neural Network
ANS	Autonomic Nervous System
ApEn	Approximate Entropy
AR	Autoregressive
BA	Bland-Altman
BMI	Body Mass Index
BP	Blood Pressure
CI	Confidence Interval
DC	Direct Current
DFA	Detrended Fluctuation Analysis
DT	Detection Threshold
ECG	Electrocardiogram
EMG	Electromyogram
FFT	Fast Fourier Transform
FIR	Finite Impulse Response
GA	General Anesthesia
GAL	Grow and Learn
HF	High Frequency
HR	Heart Rate
HRV	Heart Rate Variability
IBI	Inter Beat Interval
IHD	Ischemic Heart Disease
IIR	Infinite Impulse Response
LED	Light Emitting Diode
LF	Low Frequency
LoA	Limit of Agreement
LVH	Left Ventricle Hypertrophy
LVQ	Linear Vector Quantization
MAE	Mean Absolute Error
ME	Mean Error
MI	Myocardial Infraction
MLP	Multilayer Perceptron
MOBD	Multiplication of Backward Differences
NN50	Number of Normal Intervals with Differences more than 50 Milliseconds
OHR	Optical Heart Rate
P05	5^{th} Percentile
P95	95^{th} Percentile
PL	Powerline
pNN50	Percentage of Normal Intervals with Differences more than 50 Milliseconds
PNS	Parasympathetic Nervous System
PPG	Photoplethysmogram
PSD	Power Spectral Density
RBF	Radial Basis Function

RI	Reflection Index
RMSE	Root Mean Square Error
RMSPE	Root Mean Square Percentage Error
RMSSD	Root Mean Square of Successive Differences
RRI	R-R Interval
SA	Sinoatrial
SDANN	Standard Deviation of the 5-minute Average NN intervals
SDNN	Standard Deviation of Normal Intervals
SDSD	Standard Deviation of Successive Differences
SVD	Singular Value Decomposition
SNS	Sympathetic Nervous System
SD_1	In Poincaré plot, the standard deviation perpendicular to the line-of-identity
SD_2	In Poincaré plot, the standard deviation along the line-of-identity
Std	Standard Deviation
STFT	Short-Time Fourier Transform
TINN	Interpolation of R-R Intervals
Tn	Notch Time
Tp	Peak Time
TRI	Triangular Index
VLF	Very Low Frequency

1. INTRODUCTION

The main role of technology is to enhance the quality of life. Therefore, it is required to be affordable and have suitable outcomes especially when it comes to healthcare industry for the purpose of saving lives. Now, the healthcare industry is confronted with some major challenges such as lack of accessibility, quality, and the high costs of the medical equipment. There should be some solutions and alternatives to reduce the medical expenses for maintaining or even improving the quality of them. Moreover, there is a need that the medical equipment to be available for everyone and easy for healthcare personnel to have real-time access to patients' monitoring data. It therefore reduces the additional costs significantly if there will be more focus on preventions people from diseases instead of treating them. Wearable technology can be a suitable alternative due to its versatile and portable nature which can be safe, effective, patient-centered while it can reduce the costs at the same time [1].

In the past two decades, heart diseases such as ischemic heart diseases (IHD) together with strokes have remained the major reasons of mortalities world-wide [2]. IHD is a heart disease in which insufficient amount of oxygen and blood reach a portion of the myocardium which leads to an imbalance between the supply and demand of oxygen in the myocardium [3]. Due to not having any specific symptoms, IHD can put the life of the patient in danger and in some extreme cases it might result in the death of the patients [4]. One way to monitor IHD could be angiography which is an invasive method that could be bothersome for patients and healthcare personnel; thus, using a wearable device can be more beneficial and less cumbersome for the patient. Although ischemic events cannot directly be detected with wearable devices, research has shown that patients with IHD have different linear and non-linear heart rate variability (HRV) parameters [5] [6]. By designing a wearable device which can non-invasively monitor heart and extract related information (such as HRV), these kinds of life-threatening issues could be mitigated. This was just an example indicating that long-term measurement using wearables can be highly useful for monitoring vital organs of body such as heart.

Electrocardiography (ECG) has been the most used and common method for monitoring heart in the past decades. It is considered the “gold standard” which can provide information accurately and precisely. The ECG devices can be found in various shapes and models such as stationary ones commonly used in hospitals, the chest straps and Holter monitors which are the portable versions of ECG. While they all provide a great efficiency, some limitations are also associated with them. In case of stationary ECG devices used in hospital environments, the patients should stay in a specific position with the least possible movements while 10 electrodes are attached to different parts of their bodies. During long-term recordings in case of pre- and post-operative patient monitoring, this might become bothersome for the patients. The poor attachments of the chest straps to the skin can also lead to the generation of noisy signals.

To overcome the mentioned limitations, a wearable device is required which can be easy to use and provide comfort for long-term recordings, be able to reduce the medical expenses and be reliable in terms of data recording. Optical heart rate (OHR) technology can be a suitable alternative and embedding this technology in a wristband can have benefits for both patients and healthcare personnel. HRV information recorded by OHR could potentially be used to recognize post-surgery complications and deterioration of patient status. My motivation for this thesis was to compare the long-time data collected by OHR and ECG.

The main objective of this thesis is to evaluate if OHR technology could be an effective tool for post-operative patient monitoring. More specifically, to evaluate the beat-to-beat accuracy of OHR and to evaluate the accuracy of OHR for estimating HRV parameters. Another objective is to investigate the effect of ectopic beat removal methods on final error.

The whole content of this thesis is associated with ECG, photoplethysmogram (PPG) technology, and HRV; therefore, during the theoretical background, one chapter is devoted to each one of them. It is then followed by Chapter 5 where the methods of data processing and utilized materials for data recording are explained. The results of the thesis are demonstrated in Chapter 6 and in the same chapter, the obtained results are discussed. Finally, a summary of the whole thesis is provided in Chapter 7.

2. HEART AND ARRYTHMIAS

The cardiac diseases can be manifested as arrythmias and some of them might not have any symptoms such as tachyarrhythmias triggered by acute coronary events [7]. Therefore, screening and monitoring of heart continuously can provide useful information regarding the status of heart and the generated signals from it. Multiple techniques have been utilized in the past years for monitoring of heart. Electrocardiography is one of them.

2.1 Electrocardiography

Electrocardiography (ECG) is the most common way to record the signals generated by heart [8]. In each cardiac cycle, an electrical signal is generated which contains peaks and valleys. The whole signal is composed of 5 peaks and valleys called P, Q, R, S, T. The analysis of the ECG signal is highly dependent on the extraction of QRS complex, P and T waves. The excitation of the ventricles is represented by QRS complex and the time differences between R-peaks is called HRV. Also, some premature contractions which are not originated from sinus node could be present in the ECG signal. A normal heart usually has some stable characteristic such as the intervals between P-R or Q-T which are normally between 0.12 to 0.2 seconds for P-R and 0.42 seconds for Q-T [9]. Different features of the ECG signal such as QRS complex can be helpful with diagnosing cardiac arrythmias. In Figure 1, the ECG waveform containing P, Q, R, S, T is depicted.

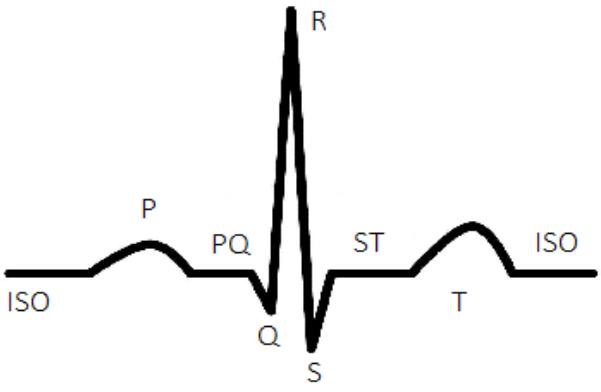

Figure 1. *ECG signal. ISO is the isoelectric line or baseline which does not have any electrical polarities. P-wave is the depolarization of the atria in response to SA node triggering. QRS complex is the depolarization of the ventricles. T wave is the ventricular repolarization. [10].*

2.2 ECG recording techniques

The ECG recording is commonly based on 12-lead electrocardiogram. It starts by placing 10 electrodes on the surface of the skin in different parts of the body. By production of heartbeats during activities of myocardium, 12 views of its electrical activity can be obtained using 12-lead electrocardiogram. The formation of the ECG signal and the interpretations regarding the time and voltage properties of the signal are valid only if the placement of the electrodes on the body skin follows the “standardized methodology” which is already determined. Following a standardized methodology will allow to have accurate comparison between different recorded ECGs in various situations and healthcare personnel. It also permits to track the changes over time and evaluate the responses of treatments to the ECG signal [11].

At first, there are four limb electrodes which should be placed in four areas of body such as right arm, left arm, right leg and left leg. The electrode on the right leg is utilized as the earth connection. The correct placement of electrodes on limbs is the extremities of the limb and for minimizing the effect of motion artifacts, it would be a good idea to attach the electrodes when the muscles of the patients are in the natural resting position. Any surface of the limb such as posterior, interior and lateral can be used for the placements of limb electrodes. In case of the leg limb, placement of the electrodes to the posterior would be difficult compared to other sides. Limb electrodes include RA (right arm), LA (left arm), RL (right leg), LL (left leg) which are placed on right arm near the wrist, left arm near the wrist, right leg near the ankle and left leg near the ankle, respectively. As well as 4 limb electrodes, there are also 6 chest (precordial) electrodes which are called V1, V2, V3, V4, V5, V6. V1 is placed to the right of the sternal border and V6 is placed over the fifth intercostal space at the mid-axillary line. V2, V3, V4 and V5 are placed within V1 and V6 [11].

2.3 ECG electrodes and electrolytes

The outer layer of skin is dry and has high electrical impedance. High impedance of the skin prevents the electrical current from flowing throughout the skin. Suitable skin preparations and electrolytes can reduce the impedance and boost the flow of ionic current through skin. The electrodes are attached to a preamplifier which measures the voltage of the metal electrodes. It can be the difference between one electrode and voltage average of other electrodes. Based on Ohm law ($V = I \times R$), less resistance against the electrical current results in a better signal quality. The used electrolytes for ECG are usually free ions such as chlorine (Cl-) and sodium (Na+) ions. They increase the conductivity; however, the high concentration of electrolytes might irritate the skin [11].

ECG electrodes can be reusable or disposable (single use). Currently, the disposable electrodes together with solid gel electrolyte are being used for ECG recording. An ideal electrode should have a good conductivity, attach to the surface of skin properly, be removed from skin easily, reduce the impedance at the skin-electrode interface and does not cause any skin irritations [11].

2.4 QRS detection in ECG signal

QRS is the most important part of the ECG waveform and provide information regarding heart rate (HR), HRV and can be used as a mean for developing automated ECG analysis algorithms. Recently, different techniques have been adopted to develop algorithms for QRS detection. These algorithms can be in the fields of artificial neural networks (ANN), filter banks, wavelet transforms, heuristic methods, and genetic algorithms [12].

In most QRS detection methods, there is a need to filter the signal beforehand. The filtering process should include removing the incoupling noise and baseline drift. For removing baseline drift, there is a need for a high-pass filter while for incoupling noise removal and attenuation of P and T waves, a low-pass filter is required [12].

2.4.1 Derivative based algorithms

This method is based on the usage of characteristics of the QRS complex such as the steep slope of the R-peak. Therefore, a differentiator such as a high-pass filter can be utilized. There are various choices for the differentiator filters. First and second derivatives-based

algorithms have been used for QRS complex detection and estimating the duration of QRS. The first and the second derivatives of the ECG signal will produce square shape pulse wave at the place of QRS complexes and the duration of the pulses are proportional to the duration of QRS complexes [13].

2.4.2 Algorithms based on digital filters

It is possible to use sets of filters for QRS complex detection. A non-linear median filter has been used in order to smooth the ECG signal in a way that there is no sign of R-peaks anymore. Then the filtered signal was subtracted from the original ECG signal which resulted in the removal of baseline drift. Finally, a simple R-peak threshold detection was applied [14]. The effect of use of four finite impulse response (FIR) band-pass filters has been evaluated and QRS complexes were classified by the help of a detection threshold (DT) [15]. Concerning QRS complex detection using filters, multiplication of backward differences (MOBD) can be utilized which provides more information regarding the occurrence of QRS complexes [16].

2.4.3 Wavelet-based QRS detection

The result of wavelet transform is a time-series representation of the function $f(t)$ which uses set of analyzing functions. A method was proposed for QRS complex detection as well as P and T waves based on wavelet transform. According to M. Bahoura et al. the advantage of detecting QRS complex together with P and T waves would be helpful in terms of tachycardia and long QT syndrome recognition [17]. ECG signal has a time-varying morphology, and it has been found out that the wavelet-based algorithms exhibit a sufficient performance and robust response to noise in the ECG signal [18]. Wavelet transform-based QRS complex detection could have good capabilities of distinguishing different parts of the ECG waveform such as QRS complex and P and T waves as well as making difference between the ECG components and the extreme noise and baseline drift [19].

2.4.4 QRS detections based on neural networks

Artificial neural networks (ANN) have been widely utilized in the fields of non-linear signal processing. The most frequently used approaches of ANN are linear vector quantization (LVQ), radial basis function (RBF) and multilayer perceptron (MLP). The ECG signal has a non-linear characteristic derived from a non-linear system (human body). Applying a linear adaptive filter for QRS detection could have some limitations and result is not always optimal. ANN has a non-linear nature and therefore is an appropriate approach for non-

linear signals and systems [20]. Supervised learning and competitive learning such as grow and learn (GAL) and Kohonen networks are mostly utilized for the purpose of “signal classifications” or specifically “QRS detection”. In a study by Z. Dokur et al., GAL was found to have the best performance among other competitive learning methods for R-peak detection [21].

2.5 Ectopic beats

Heart starts beating from SA node which is a primary source pacemaker throughout the whole heart. There are also other pacemakers together with SA node which are usually rejected as the source pacemaker during the refractory period of heart cells [22]. However, in some cases, some electrical impulses might be generated by other pacemakers which results in the generation of ectopic beats. Under this circumstance, a premature beat is arisen and the next beat after that would be a normal beat; however, the interval between the premature beat and the normal beat is longer than a normal distance. These long distances in QRS complex will generate sharp transients in HRV and can affect the result negatively especially when it comes to power spectral density (PSD) estimation of HRV [22].

Ectopic beats can be in different types. Sometimes the SA node is not reset by ectopic focus location which leads to the creation of an ectopic beat in the place of the missed normal beat. It is then followed by a normal beat again. By removing the ectopic beat, the distance between two adjacent beats will become twice as long as the mean of R-R intervals. The solution would be inserting an intermediate beat instead of the missed beat to have good quality PSD estimate [22]. The application of suitable ectopic beat removal methods reduces the error of different HRV parameters such as SDANN (standard deviation of the 5-minute average NN intervals) in time domain as well as LF and HF in the frequency domain [23].

2.6 ECG accuracy

In general, the 12-lead ECG recording principle is not always accurate and there might be inaccuracies in terms of factors associated with patients such as respirations patterns, the effect of everyday meals on the recorded ECG signal, body habitus and gender. There are also factors associated with practitioners and healthcare personnel such as incorrect attachment of electrodes to the skin or inappropriate skin preparations [11]. The artifacts can also affect the quality of ECG signals negatively.

- ## Artifacts affecting ECG signal

  The artifacts affecting ECG signal can be baseline wandering, powerline interference, EMG noise and motion artifacts.

- **Powerline Interference:** It is a 50/60 Hz frequency noise which is flowing in the lead wires. Then the corresponding noise is transferred to body which is later also available in the ECG signal and should be removed before further processing. There is a need for a filter which is capable of removing powerline interference without affecting the neighboring frequency components. Basic analogue filters might affect the ECG components near the PL frequency. Other methods of PL frequency removal such as notch filters which are digital filters can be insufficient if the deviation of frequency of the interference is too large, and adaptive filters might generate transient response time which could be unacceptable. Subtraction procedure can be a suitable method for PL frequency noise removal without affecting the spectrum of the signal and it has been tested on different ECG signals and has provided desirable outcomes [24].

- **Baseline Wandering:** In an ideal case, the baseline of the ECG signal should be at the same level compared to the isoelectric level. The skin-electrode impedance keeps changing according to the changes of the respiration volume and in the long run it results in the wandering of the ECG signal baseline compared the isoelectric level. By using a suitable filter having an appropriate cut-off frequency, this problem can be solved. In order to remove the baseline wandering and at the same time maintaining the low frequency components of the ECG signal, there is a possibility to use a cascade adaptive filter. This method works based on the detection of QRS complex to preserve the signal components which are in correlation with QRS complex, so the extremities of the signal should be already known [25]. Decompositioning the ECG signal and then reconstructing it again would be another method for coping with baseline wandering; however, the signal should be filtered beforehand which requires a prior knowledge of the R-R intervals [26]. The combination of discrete Mayer wavelet filter with cubic spline estimation has been used for baseline wandering removal. Using cubic spline, the baseline of the ECG signal is estimated, and it is subtracted from the raw ECG signal. This is a time

domain non-linear approach [27]. Kalman filter and window moving averaging are two methods of baseline wandering removal which do not require a prior knowledge of the signal [28].

- **EMG noise:** The movements of any muscle in our body can generate a signal which is called electromyography (EMG) signal. The frequency range of the EMG signal is almost similar to the range of the ECG signal which leads to their interference. The presence of the EMG noise in the long-term recordings might cause some problems while in short-term measurement its effect can be ignored. Applying a wavelet filter and choosing appropriate thresholds for that could be one approach to remove the effect of motion artifacts and EMG noise in the ECG signal [29] [30]. The other methods for EMG noise removal could be Hopfield neural networks [31], Savitzky and Golay (S&G) filters by choosing appropriate thresholds [32] and transfer domain windows such as time-frequency plane Wiener [33] and singular value decomposition (SVD) filters [34].

- **Motion artifacts:** The motion of the body can move the electrodes attached to the surface of the skin and results in a noise in the ECG signal. The whole sets of electrodes together with body skin can be modeled as sets of resistors and capacitors and any movements of body can affect the related parameters which results from the changes of the impedance between the electrodes and the surface of the skin. In long-term recordings it can affect the ECG signal negatively as it highly overlaps with the ECG signal in 1-10 Hz frequency range.

3. PHOTOPLETHYSMOGRAPHY

PPG is an optical method for measuring the propagation of light from tissues when they contain different amounts of blood in each phase of the cardiac cycle. PPG is non-invasive, low cost and easy to use. The general PPG measurement technique is based on emitting light to tissues and getting the light back after propagation from the tissue. The whole procedure starting from emitting light from the source which is a light emitting diode (LED) to its detection through photodetectors and obtaining signals, is often modeled by Beer-Lambert law. Based on this law, the intensity of light in a homogenous medium is dependent on factors such as length of the light path I and light absorption coefficient α. Equation (1) presents Beer-Lambert law and I_0 is the primary intensity of light; the one which is emitted to the medium in the first place:

$$I = I_0 e^{-\alpha l}, \tag{1}$$

If there are several substances such as skin, blood etc; light is absorbed by each of them and the effect of each one can be summed up together to obtain the final values of I. Beer-Lambert law is used for homogenous mediums. Biological tissues and blood are not homogenous due to the changes in number of blood cells in different cardiac cycles leads to the non-linear absorbance of light.

On each heartbeat, blood is pumped through the vessels in all parts of body. This will lead to the changes in the geometry and properties of the mediums (such as arteries). These changes affect the way that light is absorbed and scattered via blood cells and the variation of the light intensity can later be displayed by PPG signal. The whole PPG signal is composed of two main components which are alternating current (AC) and direct current (DC). These two terms are used in electrical engineering where AC refers to the voltage changing to different values and DC is the static voltage. In a PPG signal, pulsatile arterial blood is the AC component, and the DC component is the constant light absorption which is not always constant in reality and it has some small alteration by heart beats. When it comes to the detection of the light through photodetectors, two types of pathways could be utilized for this procedure. These two pathways are “transmissive” and “reflective”. In the transition mode, the light passes through the tissue and the detector which is attached to the other

side of the tissue receives the light. This way light collection is not possible for getting the PPG signal in some specific locations of body such as forehead or ankle where light is fully absorbed through the tissues. The reflectance pathway is mostly used for PPG applications where the detector and the light source are placed on the same side close to each other.

The wavelength of the emitted light plays an important role regarding absorption or extinction of the light through different constituents of the tissues. One of the constituents of the tissues is water (H_2O) and light can be transmitted through that efficiently if its wavelength is less than 950nm. Out of other constituents of the tissues, melanin absorbs the lights which have wavelengths less than 500nm, which means that the lights having less than 500nm cannot be effectively detected by the detectors and they are mainly absorbed by the melanin of the tissues. The concentration of melanin is different based on various types of skin pigmentation. The associations of skin tone pigmentations with the accuracy of measurements have been evaluated. Based on Fitzpatrick skin tone scale, there are 6 types of variations of skin tone which differ based on the concentration of melanin in the skin tissues. It was shown that the coverage of reliable heartbeats of the OHR device compared to an ECG reference reduced slightly for the 5^{th} and 6^{th} grade of Fitzpatrick scale. The other wavelengths of the OHR device might provide different accuracies which should be further investigated [35].

The main constituent of blood is hemoglobin (Hb) and based on its binding with oxygen can be categorized into two forms of functional and dysfunctional hemoglobin. The functional hemoglobin is called oxyhemoglobin and it is saturated fully with oxygen and in the blood of healthy people there are mostly the functional type of hemoglobin. In order to choose the wavelength in a way that the light is not absorbed by melanin and scattered by water molecules, the range of that could be varied from 510 to 920 nm. This range is equal to the wavelengths of green lights and infra-red lights, respectively. A research has shown that the green light has some benefits compared to the red and infra-red light due to AC/DC component ratio [36]. The longer wavelengths are able to penetrate to deeper parts of the tissues; and this can lead to the generation of more complex signals due to the effect of scattering in deeper parts of the tissue.

LED is used as the source of the light due to its small size and efficiency. As the detectors it is possible to use photodiodes, photocells and phototransistors. The detected signal from

the light sensors will be then preamplified, filtered and set to a specific sampling frequency which is usually in the range of 20 - 100 Hz.

As mentioned before, the PPG signal is composed of DC and AC components. Several features can be then extracted from DC and AC components. The DC component is the static part, and it determines the pulse foot (the bottom part of the signal). The AC component is the wave of the PPG signal, and it is not totally unique (the shape of cycles is not similar to each other); however, the overall pattern of the signal is closely similar which starts by a sharp rise in the beginning of the signal and ends by a decrease in the levels of the amplitude. The features that can be extracted from the AC components of PPG signal can be used to calculate HRV parameters. Pulse intervals themselves can be detected using different fiducial points in the PPG signal.

3.1 Measurement site

Based on targeted applications, there are different possibilities for choosing the most suitable site for the measurements. In the transmission mode where the detector is placed on the other side of the LED, the measurement sites could be the tissues which have less thickness such as earlobes or fingertips. In the reflectance mode, there are various choices for measurements sites such as wrist, forearm, forehead and torso [37] [38] [39]. One major difference between these two modes is that there is a need for cuff in transmission mode which pressures the arteries and leads to the prevention of venous oscillations. The anatomical features of different sites of the body also plays an important role in the formation of the PPG signal as they have different features such as different amounts of fat, muscles, tendons, arteries etc. in order to reduce the effects of motion artifacts on the PPG signal, forearm can be a good choice for the measurement site compared to wrist [40] while wrist can be a more comfortable choice for long-term measurements. Moreover, comparison of several potential measurement sites has concluded that pulse spectral power of PPG is the highest when the measurement site is finger and it is lowest when PPG sensor is attached to the forearm [41]. Different measurement sites can result in different PPG signal waveforms characteristics such as pulse peak time (Tp), dicrotic notch time (Tn), and the reflection index (RI). These characteristics are usually used for the evaluation of arteries property under different physiological conditions. They can also be utilized for diagnosing cardiovascular diseases. By choosing finger as the measurements site, it is more convenient to extract Tp, Tn and RI from PPG. Tp and RI is much smaller when the measurement site

is finger compared to other measurements sites such as forehead, forearm, earlobe and wrist, and the mean amplitude of the PPG signal is higher in this case [42]. Measurement site can be chosen in a way that it is less prone to motion artifacts caused by movements. Choosing forearm as the measurement site reduces the estimation error as it is less influenced by motion artifacts [36].

3.2 Factors affecting the quality of the PPG signal

Factors can be categorized into three groups such as sensing factors, biological factors and cardiovascular factors. The factors associated with sensing could be the characteristics of the light emitted from the LED, the photodetector which is responsible for collecting the light, the coupling effect between skin and the sensor. The design and the geometry of the sensor should be in a way that minimizes the effects of the ambient light on the PPG signal. The distance between the photodiode and the LED should also be taken into consideration. The best distance between the LED and the photodiode for infra-red and green light can be 6 to 10 mm and 2 mm [43], respectively. The biological factors could be some innate characteristics of the tissue such the skin pigmentation and cardiovascular factors could be the position of body, age, the stresses applied to the vessels which leads to the alterations in the flow of the fluids etc.

Moreover, the motion artifacts can have profound effects on the quality of the PPG signal and therefore it is needed to be removed or at least minimized their effects. There are usually three different types of motion artifacts affecting the PPG signal:

- **Tissue modifications due to movements:** Any movements of the tissues whether they are intentional or non-intentional can affect the status of the shape of the fat and other inner cells of the tissue. It will then result in the light that is being received by the photodiode and alters the shape of the PPG signal. The reasons for creation of these types of artifacts could be the location of the PPG sensor implanted on the tissue such as writs, earlobes, forearm etc. (for example, the implementation of the PPG sensor in earlobes is less prone to the creation of movement artifacts compared to wrist) and the way the PPG sensor is placed on the tissues such as the stress of the mechanical components of the sensor to the skin or the strap responsible for fastening the PPG sensor to the tissue [44].

- **Relative motion of the sensor-skin interface:** The interaction of the surface of the skin with the PPG sensor is not rigid and it is prone to movements which can be resembled to a mass-spring system. Any movements which result in the displacement of the sensor compared to the surface of the skin can affect the light path leading to the creation of noise in the PPG signal [44].

- **Changes in the pressure between the optical probe and the skin:** The amplitude of the PPG can be altered due to the amount of applied pressure from the sensor probe to the surface of the skin. For having an appropriate interaction between the skin and the sensor probe some levels of pressure are required; however, if the applied pressure exceeds the threshold, the amplitude of the PPG signal may decrease due to squeezing the blood vessels [44].

- **Effects of skin temperature on PPG signals:** The effects of the temperature on the surface of the skin where there is a constant contact with the PPG sensor have been evaluated. The direct contact of the PPG sensor with skin generates heat and results in vasodilatation. By increasing the temperature from 34 to 45 degrees Celsius, the fluctuations of the amplitude in the PPG signal decreases significantly resulting in a more stable PPG signal. This research was done by infra-red light and the distance between the LED and photodiode was fixed to 6 mm [44].

- **Effects of the distance between LED and photodiode on PPG signal:** The distance between the light emitter and detector can affect the resulting PPG signal. As the distance between the LED and detectors increases, the light should go the longer path to reach the detector which results in the reduction of the intensity of received light. The AC and DC components of the PPG signal decrease by increasing the distance. However, the relative pulse amplitude and stability of the signal increases when the distance increases. Traveling longer distance of light by increasing the distance of emitter and detector results in higher levels of absorption of light and therefore larger plethysmograph signal. But it also leads to the decrease of the signal to noise ratio as soon as the intensity of the light decreases [45].

- **Effects of using multiple photodetectors instead of one:** The effect of increasing the number of photodiodes has also been evaluated. The use of three photodiodes instead of one photodiode increases the chances of collecting the backscattered lights more easily. Detection of larger amounts of backscattered lights leads to the larger pulse amplitude and therefore larger photoplethysmograms [44].

- **Wavelengths of the source light:** The wavelengths of the lights used as the light source can be 463nm (blue light), 543nm (green light), 571nm (yellow light), and 634nm (red light). Red light is able to penetrate in more depth of the tissue compared to shorter wavelengths. Modifying the distance between the detector and the emitter has different effects for different colors. By increasing the distance of detector and emitter, all lights will lose their intensities [44].

4. HEART RATE VARIABILITY

HRV can provide useful information regarding health status of individuals such as functionality of nervous system or determining possible heart dysfunctionalities. In QRS complex, there are alterations between the time intervals of each adjacent heartbeat called HRV which is illustrated in Figure 4 [46]. It is concluded that the reduced HRV might be a sign of cardiovascular diseases. Other areas in which HRV can provide useful information are problems which directly affect autonomic system such as diabetes [47]. HRV can be quantified with different metrics in time and frequency domain as well as with non-linear parameters [48]. In Figure 2, a part of an ECG signal is depicted and by collecting the differences between adjacent R-peaks, HRV can be obtained.

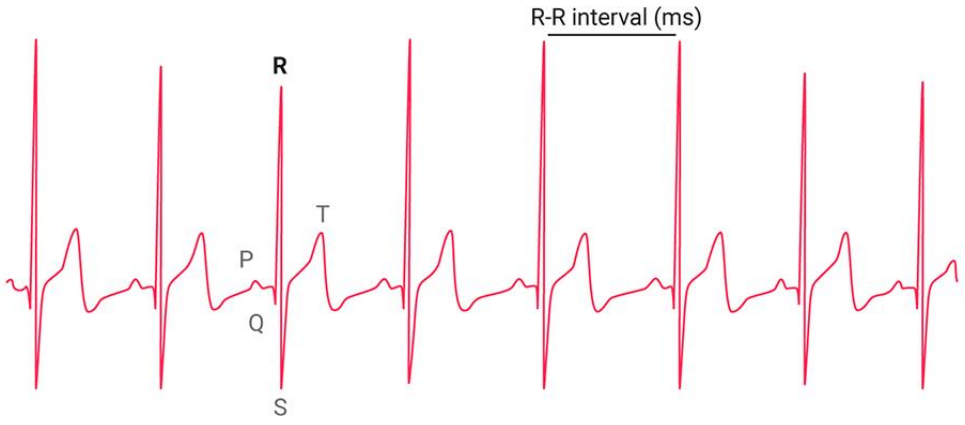

Figure 2. *HRV is derived by collecting the differences between adjacent R-peaks. Heart is not a metronome and R-R intervals differ from each other [49].*

4.1 Physiological background of HRV

HRV is regulated by autonomic nervous system (ANS). ANS is responsible for the maintenance of homeostasis which means it can for example regulate gastrointestinal responses to food, eye focus, blood pressure etc. ANS has two components: the sympathetic (SNS) and parasympathetic (PNS). Each of these components are being stimulated by different factors. In case of sympathetic component, it is affected by exercise, heart disease and stress which results in the increases of heart rate. In case of

parasympathetic component, it is being influenced by the functionality of internal organs and allergic reactions which decrease the levels of heart rate [50].

4.1.1 HRV Parameters

HRV can be quantified with different metrics in time and frequency domain as well as non-linear parameter and in total 31 HRV parameters are introduced in this thesis. Common time domain HRV parameters are SDNN, NN50, pNN50 and RMSSD. SDNN is the standard deviation of normal R-R intervals in milliseconds (ms). It can provide information about the risk of mortality and morbidity [51]. NN50 is the number of each pair of R-R intervals which have differences more than 50 ms and its percentage is described by pNN50. RMSSD is the root mean square of differences of adjacent beats.

The time domain beat-to-beat heart rate signal can be converted into frequency domain using fast Fourier transform (FFT) or autoregressive (AR) model. Common frequency domain parameters are very low-frequency (VLF) power, low-frequency (LF) power, high-frequency (HF) power and total power (TP) [52]. The range of LF band is between 0.04 to 0.15 Hz and the usual minimum window for measuring LF is 2 minutes [53]. The range of HF band is between 0.15 to 0.4 Hz and the minimum time window for measuring HF is usually 1 min. The LF/HF ratio is usually measured for long term recordings (over 24 hours) and is intended to measure the activity of SNS compared to PNS [64].

The factors resulting in the generation of HRV are not following a simple pattern like a straight line and they have a non-linear characteristic. The non-linear parameters such as SD_1, SD_2 and SD_1/SD_2 can be obtained after fitting the ellipse. The predictability of the R-R intervals can be understood using ApEn (approximate entropy) and if it has a higher value then it demonstrates a lower predictability [48].

Here are the usages of some of HRV parameters in interpreting HRV:

- **pNN50:** NN50 was first introduced in 1984 [54] to collect the number of beats which have differences more than 50ms compared to their neighboring beats. The threshold could also be a variable (such as 7% of the previous NN interval) instead of choosing a fix number (50ms). It is concluded that choosing a fix threshold would be simpler and easier for measurements [55]. pNN50 was later introduced to measure the probability of the beats having differences more than 50 ms with

neighboring beats [56] [57]. pNN50 can provide useful diagnostic and prognostic information regarding different conditions. pNN50 can reflect the activity of vagal tone [58] and the reduction of pNN50 can be associated with the risk of cardiac events [59]. For post-myocardial infarction (MI) patients, the lower levels of pNN50 could be associated with higher mortality rate [60]. People having systemic hypertension also have reduced pNN50 [55].

Having stress and doing a mental task also affects the functionality of SNS and PNS and therefore reduces the levels of pNN50 [61]. Schizophrenia which is a mental disorder leads to the reduction of vagal tone and in a study all patients dealing with schizophrenia had the percentage of pNN50 lower than 4 [62]. General anesthesia (GA) also decreases pNN50 significantly and there is no correlation anymore between pNN50 and HF components of frequency domain parameter of HRV during GA [63]. Hypertension which is a serious reason of coronary diseases and stroke are associated with ANS and hypertensive individuals have significantly reduced pNN50 [64]. The relationship between body mass index (BMI) and ANS has also been evaluated. It was shown that for non-obese adults, the BMI and pNN50 are inversely related [65].

The threshold for calculation pNNx is usually considered 50 ms. pNNx has also been measured with other thresholds other than 50 (preferably < 50) and in a study by J. E. Mietus et al. the result for different groups of patients by setting the threshold to 20 ms was more distinguishable which makes it a more suitable threshold when it comes to comparing the pNNx values of different patients' groups [55].

- **SDNN:** SDNN is the standard deviation of successive inter-beat-intervals. Age and gender can affect the value of SDNN [66]. During the analysis of patients with MI, the lower levels of SDNN were more associated with the risk of mortality [67]. SDNN is a strong predictor of mortality for some specific diseases such as amyloid light-chain (AL) amyloidosis where patients have a limited life expectancy [68]. SDNN has a good specificity and sensitivity when it comes to the detection of autonomic dysfunction [69]. Also, the effects of depression and anxiety with SDNN parameters have been evaluated. SDNN was found to be decreased in patients dealing with social phobia, panic disorder and generalized anxiety disorder; however, the reason

could be mostly due to the antidepressants that they were taking [70]. Going under surgeries such as coronary artery bypass grafting could result in the reduction of HRV parameters including SDNN. The reason for immediate reduction in SDNN could, besides the actual response of ANS, be the surgical manipulations on heart and the surrounding tissues [71]. The levels of blood glucose and diabetics have associations with SDNN, and they are inversely related. Patients having impaired fasting glucose levels have reduced levels of SDNN [72].

- **RMSSD:** RMSSD is the root mean square of differences of successive beats and an important time-domain HRV parameter which can provide useful information regarding the status of ANS. For epileptic patients it can be a good predictor of sudden unexplained death in epilepsy (SUDEP). SUDEP risk and RMSSD are inversely related [73]. RMSSD in smokers is lower than non-smokers which is due to the effect of smoking on ANS [74]. RMSSD is significantly associated with body mass index (BMI) inversely and it has been found to be significantly lower in children with obesity than children having normal weight [75].

- **The Poincaré plot:** The Poincaré plot is the demonstration of R-R intervals against the following R-R intervals. In order to prepare the plot, an ellipse should be fitted to the datapoints. The ellipse is obtained by adding two extra axes which are established at 45 degrees to the main axis. The distances of the datapoints from each of these axes are measured and their standard deviations are calculated. The obtained standard deviations SD_1 and SD_2 determine the width and length of the fitted ellipse, respectively. The width of the ellipse (SD_1) represents the short-term HRV which has a linear characteristic and highly correlated with SDSD (standard deviation of successive RR interval differences) which is a time-domain HRV parameter, and the length of the ellipse (SD_2) indicates the long-term HRV [76]. The datapoints which have placed above the line of identity, which is the length of the ellipse, are the R-R intervals that have longer lengths compared to the previous ones and the opposite applies to the ones located below the identity line [77]. It has been shown that the length and width of the Poincaré plot become wider in different states of body (supine lying, standing, exercising and following recovery) after an endurance training [78]. Figure 3 illustrates the Poincaré plot where SD_1 and SD_2 are the width and length of the fitted ellipse.

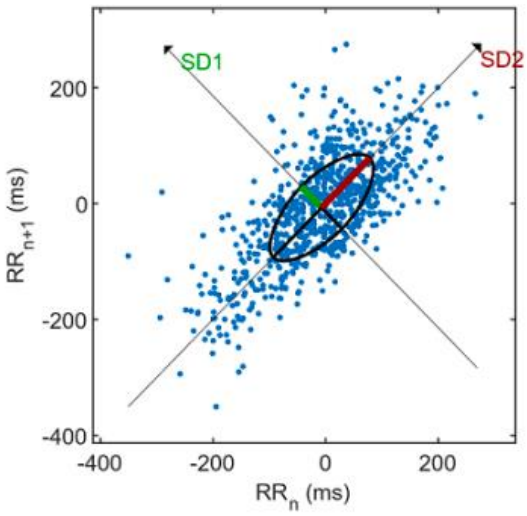

Figure 3. *This figure represents the R-R intervals VS next R-R intervals which is called Poincaré plot. SD_1 and SD_2 are the width and length of the fitted ellipse [78].*

4.1.2 Time domain vs frequency domain HRV parameters

Frequency domain HRV parameters can provide more useful information during short-term recording, and they perform better in short-term measurements compared to long-term monitoring. In general, 5-minute recording can be a suitable length for accurate measurement of frequency components of HRV [79]. The time domain parameters can also provide information for short time recordings; however, the frequency domain parameters can be interpreted more easily in terms of physiological regulations. For long term measurements, time domain parameters are preferred. The reason is that heart rate modulation is less stable during long-term recordings due to significant difference during day and night recordings. Under this circumstance, the frequency components of HRV cannot be properly interpreted [79].

Some of the frequency domain parameters have a high correlation with time domain parameters especially during long-term recordings (over 24h). The reason behind that could be mathematical and physiological relationships. For instance, SDNN, triangular index (Tri) and interpolation of R-R intervals (TINN) have correlations with TP parameter. SDANN has correlation with ultra-low frequency components and RMSSD, SDSD, pNN50, NN50, differential index and logarithmic index have a correlation with HF parameter [79].

4.2 Association of HRV with post-surgery complications

Several studies have revealed that HRV can be affected by post-surgery complications. In a study by Scheffler et al [80], 47 subjects had undergone abdominal surgeries in which 19 subjects faced complications. On the second post-surgery day, there was a decrease from 8.51 ± 4.46 (mean $\pm$ standard deviation) to 5.71 ± 2.81 in pNN50 values for subjects with complications. Ernst et al [81] showed that for patients with hip fracture, those who had post-surgery complications had a fall in RMSSD and a rise in TP and SDNN remained without any changes. In another study by Lerma et al [82], the effect of complications on non-linear parameters of HRV was evaluated and it was concluded that “complicated” group had lower SD_1 and SD_2.

5. MATERIALS & METHODS

5.1 Materials

In this section, the recruited subjects and study devices are introduced.

5.1.1 Subjects

There were altogether 31 selected subjects for this study. There were 17 females and 14 males. The median age and BMI were 71 and 27, respectively. 26 of the patients were non-smokers. They had undergone gastrointestinal surgeries in Päijät-Häme central hospital and their HRV was recorded by both ECG reference and an OHR wristband after surgeries. The duration of recordings was varied from around 24 hours up to 72 hours for each subject. In total around 1200 hours of data was analyzed.

5.1.2 Devices

The ECG reference device was eMotion Faros 360 made by Bittium and the OHR wristband was Aino by PulseOn. The sampling frequency used for the OHR device was 25 Hz and the LED was emitting green light with wavelength of 573 nm. The sampling frequency of the ECG reference was set either 250 Hz or 1 kHz. Figure 4 displays the OHR study device for recording PPG signal.

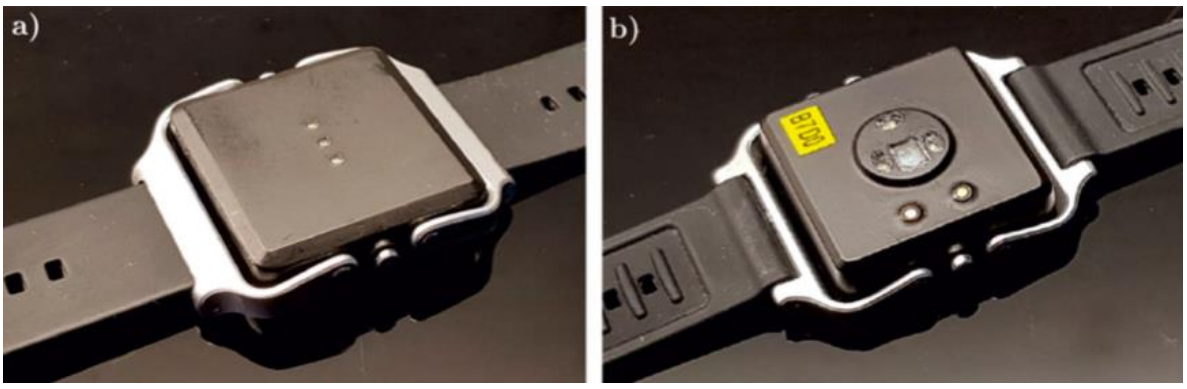

Figure 4. *PulseOn Aino used as the OHR device for recording HRV. (a) is the top view, (b) is the LEDs and photodiode side [84].*

5.2 Methods

The methodology used in this thesis consists from a set of data processing steps and algorithms for analyzing the recorded signals. In Figure 5 different steps of the methodology are depicted.

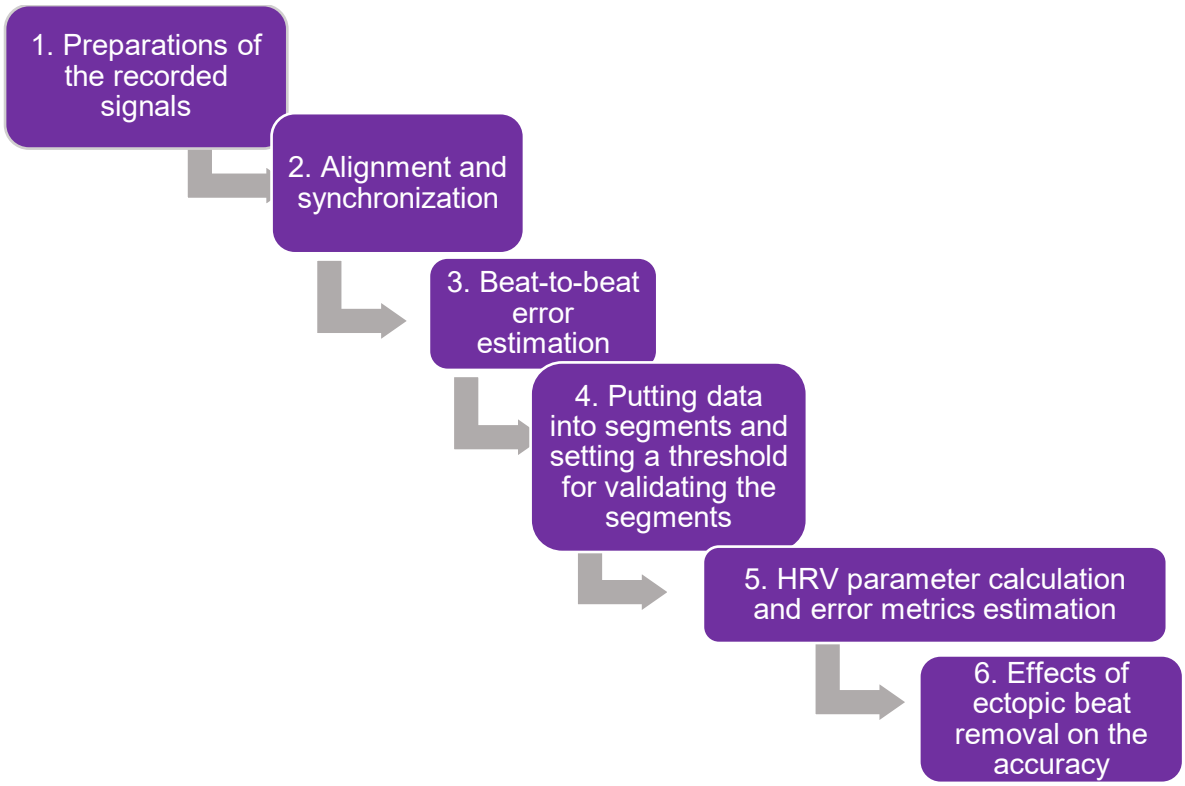

Figure 5. *The main steps involved in the methodology of this thesis. The signal preparation in step 1 is the filtrations of the signals and R-peaks extraction. Step 3 includes the introduction of different error matrices used in the thesis work. In step 5 there are HRV parameters calculations in different time and frequency domains as well as non-linear ones and error metrics are calculated.*

The whole signal processing from steps 1 to 6 in the thesis work was done by MATLAB_R2019b and Python.

5.2.1 Preparations of the recorded signals

The signals that were already obtained from the ECG reference device contained noise (high frequency noise due to power line interference and baseline wandering) which could have been affecting the accuracy of final result negatively. As a result, prior to any further data processing, it was required to minimize the effects of these noises available in the ECG data. Concerning the filtrations of the ECG raw signal, the baseline wandering was removed using a median filter having 100 ms length and subtracting the median value of ECG signal from the original signal. This was done in order to enhance the accuracy of R-peak extraction in the next step. Figure 6 displays the ECG signal before and after the removal of baseline wandering.

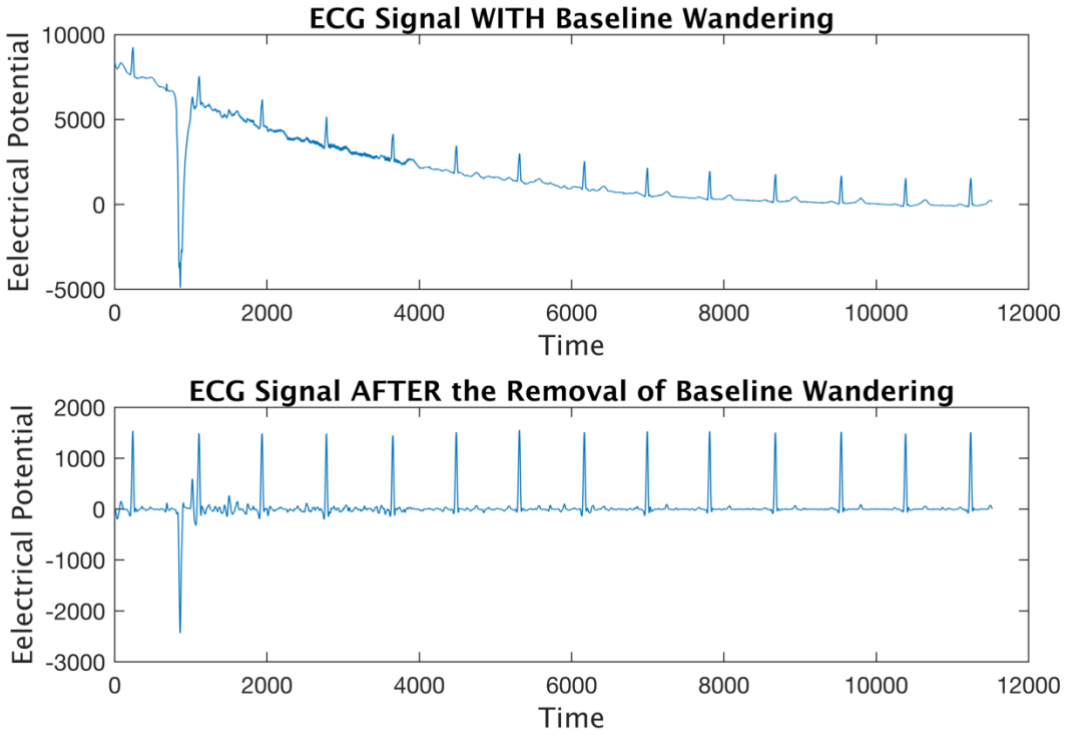

Figure 6. *Removal of baseline wandering. The upper figure is the ECG signal containing baseline wandering and it is removed in the bottom figure for the improvement in R-peaks extraction in the next step.*

Apart from the baseline wandering, there is a “high frequency” noise due to power line interference which can be properly removed using a low-pass infinite impulse response (IIR) filter having cut-off frequency equal to 40 Hz (order = 4) and forward-backward filtering.

The preprocessing stage was then followed by the detection of R-peaks for preparation HRV. There are different methods for QRS complex detection such as Pan-Tompkins which is based on suppressing the P and T waves and its algorithm also contains the filtering process [83]. 'findpeaks' is an inbuilt function on MATLAB which takes sets of parameters as the input to find the R-peaks. The performance of the function was quite efficient and therefore it was mainly utilized for this thesis. The variables that 'findpeaks' takes as the input are the sampling frequency of the ECG signal, the minimum height of the R-peaks and the minimum width of the two-consecutive R-peaks that are going to be detected. The detected R-peaks were then visually checked for confirmation. An example of pre-processed ECG with detected R-peaks marked with red circles is illustrated in Figure 7.

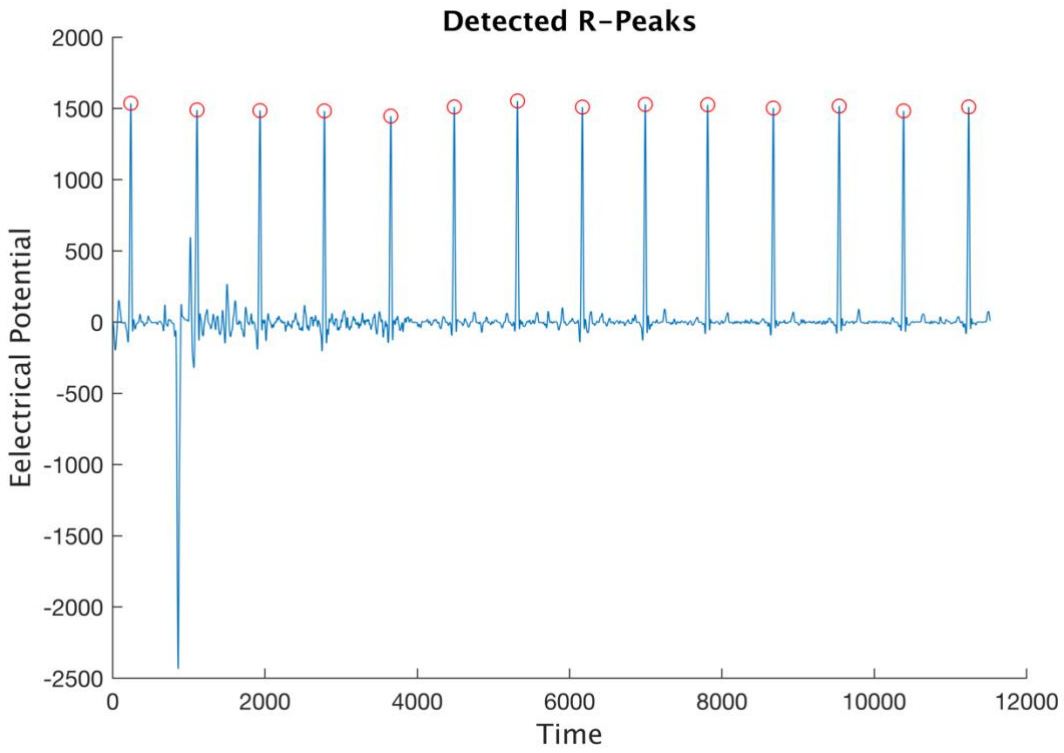

Figure 7. *ECG signals with detected R-peaks marked by red circles.*

After extracting R-peaks, the time difference between each two beats was calculated which represents the HRV and it is called RR tachogram. Next, the time vectors of ECG RRIs and PPG IBIs were created. Inter-beat-intervals estimated with PulseOn proprietary algorithms along with a signal quality estimate for each beat was directly saved and therefore there was no need for calculation of peak/heel distance in the PPG signal. The time vector of the IBI

signal is saved in timestamp format. The low-quality recorded beats caused by patients' movements were removed prior to any PPG IBIs signal processing.

5.2.2 Further filtration and ectopic beats

A threshold was set to remove the beats which values were significantly higher or lower compared to the mean of previous beats [84]. The HRV can be further processed by detecting the ectopic beats and removing them. The algorithm proposed by Thuraisingham [85] for the detection of ectopic beats is provided in Equation (2). Prior to applying the ectopic beat detection method, the RR tachograms were detrended to have a steady baseline.

$$D(n) = \frac{|S(n) - S_m|}{1.483 med\{|S(n) - S_m|\}}, \quad (2)$$

$S(n)$ denotes the RR-intervals and S_m is the median value of the RR-intervals. $D(n)$ which is a vector, contains numbers ranging from very small values (close to zero) to higher values. The bigger $D(n)$ is, the more IBIs are deviating from the main trend of the signal. The threshold proposed by Thuraisingham for ignoring ectopic beats was 4.

5.2.3 Synchronization and alignments

Up to this stage of signal processing, four vectors including the ECG RRIs, PPG IBIs and their corresponding time vectors have been constructed. The ECG device and the OHR wristband were using different internal clocks which resulted in a time drift especially during long-term recordings. Therefore, the time drift was compensated to make the beat-to-beat error estimation between ECG RRIs and PPG IBIs possible. In some cases, the synchronization needed to be repeated in different segments of the HRV as they sometimes went out of sync in long-term recordings.

5.2.4 Beat-to-beat error estimation

After proper synchronization and alignment of the ECG RRIs and PPG IBIs, it was possible to compare IBIs with each other. This comparison between each two corresponding beats could be represented by different error metrics such as mean error (ME) or bias, mean absolute error (MAE), relative mean squared error (RMSE) and their percentages (MAPE and RMSPE, respectively) as well as the standard deviation of mean error.

The equations for different error metrics are as following:

Mean error (ME):

$$ME = \frac{-1}{n}\sum_{i=1}^{n}(y_i - x_i), \quad (3)$$

In Equation (3), the values of y are heartbeat intervals produced by the OHR device. n is the total number of beats. In this thesis, the number of beats detected by the OHR device was generally less than the number of beats detected by the ECG reference, so the number of paired IBIs were equal to the number of beats recorded by the OHR wristband. The other variable x provides the data points of the reference measurement method. The subtraction of each paired IBIs divided by the number of all paired IBIs results in the calculation of mean error which can have positive or negative polarity.

Mean absolute error (MAE):

$$MAE = \frac{1}{n}\sum_{i=1}^{n}|y_i - x_i|, \quad (4)$$

Similar to ME calculation, MAE provides the average of difference between two measurement data; however, in MAE, the absolute values of differences are calculated which always results in a positive number as MAE.

Mean absolute percentage error (MAPE):

$$MAPE = \frac{100}{n}\sum_{i=1}^{n}|(y_i - x_i)/y_i|, \quad (5)$$

The differences between the paired IBIs are first divided by the values of the reference measurement. At the end, the final value is multiplied by 100 to demonstrate it in percentage.

Root mean square error (RMSE):

$$RMSE = \sqrt{\frac{1}{n}\sum_{i=1}^{n}(y_i - x_i)^2}, \quad (6)$$

In RMSE, the average of squared differences is measured, then the second root of that is calculated.

Relative mean square percentage error (RMSPE):

$$RMSPE = 100\sqrt{\frac{1}{n}\sum_{i=1}^{n}((y_i - x_i)/y_i)^2}, \quad (7)$$

The differences between paired IBIs are divided by the values of the reference device. Then the average of squared differences is measured. The final value is in percentage.

Standard deviation of differences (Std):

$$\sigma = \sqrt{\frac{1}{n}\sum_{i=1}^{n}(x_i - \mu)^2}, \quad (8)$$

X_i is the set of differences between the ECG RRIs and PPG IBIs which are subtracted by μ which is the mean of the differences.

In addition to the previously mentioned error metrics, e20 and e50 are defined which are the number of paired IBIs having less than 20 ms and more than 50 ms mean error, respectively.

5.2.5 Preparation the data for HRV analysis

As it was mentioned in the previous chapter, one way to evaluate the performance of OHR was comparing each beat of PPG IBIs with each beat of ECG RRIs. To obtain more information regarding the performance of OHR devices, the HRV parameters obtained from OHR and ECG were compared with each other. The signals were divided into segments and

the duration of each segment was chosen as 5 minutes. In each segment there were various number of beats and in order to make sure that the quality of each window was sufficient enough for being compared with the ECG reference, a threshold was then chosen to ignore the segments in which there were not enough number of beats as described in the next section.

5.2.6 Choosing segments having enough IBIs

In this thesis, the threshold was set based on the length of windows. The length of each window was 5 minutes and if the sum of the duration of IBIs in each was equal to the 80% of the length of the segments, then that window was being accepted. In each set of data, setting the threshold to 80% of the length of each window would result in the acceptance of different number of segments based on the quality of the recorded PPG signal which was later displayed as the coverage in the results section. The error metrics were then represented by comparing the corresponding segments with each other and also comparing individuals with each other.

5.2.7 HRV parameter calculations

Linear and non-linear HRV parameters were calculated for each segment. Each type of parameters could provide specific information regarding ANS and the measurement error could be varied for different parameters. In this thesis, calculated HRV parameters are listed in Table 1[1].

Table 1. *HRV parameters in time and frequency domain as well as non-linear parameters which were utilized in this study.*

Time Domain Parameters	
SDNN	standard deviation of NN intervals
RMSSD	root mean square of successive differences
pNN50	percentage of intervals having more than 50 ms difference
NN50	number of intervals having more than 50 ms difference
IQR	The middle spread of IBIs
Median	median of IBIs
Mean RR	mean of IBIs
Kurtosis	kurtosis of IBIs

[1] The HRV parameters open-source code can be found at:
https://github.com/MarcusVollmer/HRV/blob/master/HRV.m

Variance	variance of IBIs
Mode	mode of IBIs
HR Mean	mean of heart rate
TRI	triangular index
TINN	triangular interpolation of NN intervals
Frequency Domain Parameters	
VLF Abs	very low frequency absolute power
LF Abs	low frequency absolute power
HF Abs	high frequency absolute power
LF Norm	LF normalized power
HF Norm	HF normalized power
VLF Log	natural logarithm of VLF absolute power
LF Log	natural logarithm of LF absolute power
HF Log	natural logarithm of HF absolute power
VLF Rel	VLF relative power
LF Rel	LF relative power
HF Rel	HF relative power
LF/HF	LF power to HF power ratio
Non-linear Parameters	
ApEn	approximate entropy
SD_1	in Poincaré plot, the standard deviation perpendicular to the line-of-identity
SD_2	in Poincaré plot, the standard deviation along the line-of-identity
SD_1/SD_2	ratio of SD_1 to SD_2
DFA α_1	short-term fluctuation slope of detrended fluctuation analysis
DFA α_2	long-term fluctuation slope of detrended fluctuation analysis

The HRV parameters mentioned above were calculated for all subjects in 5-minute segments.

5.2.8 Error measurement of HRV parameters

The same error metrics than in section 5.2.4 were used for HRV parameters here again. Instead of the differences between paired IBIs, the differences between corresponding segments were used. In addition, two new parameters: 5^{th} percentile and 95^{th} percentiles of the relative error were also evaluated. They were the values of relative error that 5 % and 95 % of the data lies below them, respectively.

5.2.9 Presentation of similarities

Scatter plot and Bland-Altman (BA) plot can visualize the similarities and provide information for two groups of data. As we also had two sets of data in this thesis, the agreement could be assessed using these methods. Scatter plot can provide relationship between two variables and BA plot can tell regarding the differences between the two methods. Scatter plot, which is a statistical technique, can say how much the two data sets are related with each other and it can be determined using coefficient of determination (r^2) which can be varied from 0 to 1 and the more it is closer to 1, the more correlation is between the two data sets [86].

In BA plots, the x-axis represents the mean of methods A and B and the y-axis is represented by the differences between the methods A and B. The BA plot contains at least three horizontal lines indicating the upper and bottom limits of measurements as well the mean value of differences. It is expected that 95 % of data points are within the limits of agreement (LoA). The LoAs are calculated using Equation (9).

$$LoR = bias \pm 1.96 * Std, \tag{9}$$

where bias is the average of differences between two methods and Std is the standard deviation of differences [87].

Confidence intervals (CI) can be defined around three horizontal lines of upper and bottom LoA and mean. Previously, the 95 % LoA was calculated by Equation (9), 95 % confidence intervals were then calculated using Equation (10).

$$95\%\ CI\ of\ bias = bias \pm t_{\left(n-1,1-\frac{\alpha}{2}\right)} * \left(\frac{S_d}{\sqrt{n}}\right), \tag{10}$$

In Equation (10), ***bias*** is the average of differences of measurements, n is the population, and, in this thesis, it was either the number of patients or segments, α is 0.05 if 95 % of confidence intervals is required, t is the t-test and S_d is the standard deviation of differences. 95 % CI of upper and bottom LoA is obtained by Equation (11):

$$95\%\ CI\ of\ LoA = LoA \pm t_{\left(n-1,1-\frac{\alpha}{2}\right)} \sqrt{\left(\frac{1}{n} + \frac{1.96^2}{2(n-1)}\right) S_d}, \quad (11)$$

The variables in this Equation are similar to Equation (10).

5.2.10 Effects of ectopic beat removal on the accuracy of the measurements

The ectopic beats available in ECG signal and various noises in PPG signal such as effects of motion artifacts and ambient light could affect the accuracy of error estimation negatively. Effects of different methods of noise cancellation on final error were evaluated in this study. Two methods proposed by [85] and [84] were utilized for removing ectopic beats and other beats which were deviating so much from the main trend of the signals.

6. RESULTS & DISCUSSION

6.1 Beat-to-beat error estimation results

In Table 2, the result of beat-to-beat error estimation for all subjects is provided. The variables from left to right are: subjects, number of paired IBIs, mean error (ME), mean absolute error (MAE), percentage of mean absolute error (MAPE), root mean square error (RMSE), percentage of root mean square error (RMSPE), the standard deviation of ME, the number of IBIs which have less than 20 ms differences, the number of IBIs which have differences more than 50 ms, the coverage[2] of PPG IBIs and the duration of recorded data with either of devices. These results were obtained after applying ectopic beat removal methods and artifact correction algorithm.

[2] The PPG wristband automatically detects the IBIs which did not have good qualities and therefore they were removed before making the beat-to-beat comparisons. The "IBI coverage" in Table 2 refers to the percentage of good quality IBIs to the sum of all detected IBIs. Properly fastening the wristband can improve the result in this section.

Table 2. *The error metrics for 31 subjects are provided in this Table. The Table contains information regarding the paired IBIs, ME [ms], MAE [ms], MAPE [%], RMSE [ms], RMSPE [%], standard deviation of ME, e20 (number paired IBIs having less than 20 ms absolute difference), e50 (number of paired IBIs having more than 50 ms absolute difference), IBI quality (percentage of good quality beats over all detected beats) and the duration of recordings.*

P.No	Paired IBIs	ME [ms]	MAE [ms]	MAPE [%]	RMSE [ms]	RMSPE [%]	Std [ms]	e20 [ms]	e50 [ms]	IBI coverage	PPG duration [h]	ECG duration [h]
1	55393	-3.46	11.86	1.14	30.24	3.19	30.04	50451	2222	59.20	71.7	68.5
2	62511	-3.14	10.82	1.2	22.89	2.75	22.65	57763	2158	49.59	31.2	28.1
3	20327	2.77	10.62	1.14	17.66	1.89	17.44	17593	349	62.15	15.9	34.3
4	59722	1.41	10.81	1.13	25.59	2.72	25.47	54233	2253	42.76	32.8	46.9
5	192573	-4.14	7.63	0.82	16.91	2.05	16.37	181300	2318	67.52	73	70.1
6	63963	-4.67	9.1	1.09	16.15	1.95	15.41	58152	1250	53.16	26.8	25
7	125372	-1.74	10.26	1.66	19.15	3.26	19.05	111798	3788	49.81	48.4	47.1
8	38732	-5.55	10.65	1.02	23.27	2.34	22.58	35378	1211	50.26	20.1	68.6
9	57560	-6.64	13.90	1.61	25.38	2.92	24.5	47325	2042	23.13	32.8	32.3
10	183488	-4.92	9.02	1.05	17.22	2.08	16.48	168975	2719	59.63	71.8	68.5
11	60222	3.13	9.28	0.99	18.86	2.12	18.52	54676	1618	65.29	23.1	23.8
12	132359	2.64	9.66	1.13	17.07	2.02	16.78	118573	2636	59.44	51.4	47.2
13	57506	-7.53	23.01	2.3	48.01	4.91	47.31	42026	5258	63.32	24.1	23.7
14	107826	-6.43	13.45	1.31	30.04	3.05	29.32	94517	5111	60.27	48.2	46.8
15	53050	2.78	10.13	1.18	16.82	2	16.58	46619	931	56.35	22.1	22
16	177102	2.97	10.11	1.17	17.62	2.1	17.36	156739	2204	42.09	79.3	71.2
17	82793	1.73	11.44	1.48	19.64	2.66	19.56	70150	1656	36.19	49.7	48.2
18	67584	3.17	7.02	0.75	14.21	1.56	13.77	64560	895	69.80	24.2	24.3

19	17683	-3.06	7.69	1.21	12.83	2.02	12.46	16395	175	12.93	5.8	6.5
20	91461	-3.69	8.04	1.26	12.69	2.01	12.12	84602	702	60.61	27.8	48.8
21	46471	-3.8	9.84	1.13	17.09	2.07	16.56	42986	875	28.77	71.1	23.8
22	46197	2.76	9.54	1.02	18.84	2.08	18.34	42324	1360	45.78	22.4	24.7
23	137120	3.06	12.13	1.73	24.42	3.58	24.19	120473	6157	57.57	49.5	48.5
24	51585	-1.76	15.26	3.71	38.1	4.42	37.99	43014	4100	52.41	24.3	24.3
25	966	-10.2	35.74	4.84	69.47	9.74	68.7	544	157	1.65	2.2	2.2
26	101416	-3	4.54	0.66	7.89	1.16	7.29	99529	365	76.81	26	26
27	26305	-4.08	10.93	1.22	22.26	2.5	21.89	23132	831	22.79	24.7	45.1
28	122193	-3.33	13.05	1.65	24.63	3.7	24.4	102198	3257	54.95	48.6	46.8
29	111022	3.48	10.19	1.23	17.92	2.23	17.48	96351	2544	56.72	48	43.8
30	127521	-4.03	10.61	1.33	17.22	2.19	16.72	110207	2602	58.94	47.8	46.8
31	62640	4.21	9.12	1.03	20.78	2.55	20.55	57878	994	62.06	24.4	24.1
Average/Total	**2540663**	**-1.34**	**10.3**	**1.28**	**20.28**	**2.51**	**19.86**	**2270461**	**64738**	**49.63**	**1170.5**	**1209.7**

2.5 % of paired IBIs had more than 50 ms absolute difference, and 89.3 % of paired IBIs had less than 20 ms absolute difference which shows that there is a high agreement between the HRV recorded by both devices. The high accuracy of OHR for recording IBIs can be further approved by the weighted average of MAE which was 10.3 ms.

Several studies already evaluated the performance of OHR devices (by beat-to-beat comparison) in different situations. In the study by Parak et al, subjects wore an OHR wristband together with an ECG reference device at home. After ectopic beats removal and alignments of signals, mean absolute error (MAE) and mean error (ME) of beat-to-beat intervals were calculated 5.94 ms and -0.33 ms, respectively [88]. The number of subjects was 10 and the duration was 5.1 $\pm$ 1.2 hours.

Tarniceriu et al [89] calculated the error metrics for the patients who had undergone surgeries and they were recovering from anesthesia in post-anesthesia care unit. There were altogether 18 patients which were classified into two groups of sinus rhythm (SR) and atrial fibrillation (AF) group. For the SR group the MAE and RMSE were 7.34 ms and 16.70 ms, respectively. For the AF group the error was higher compared to SR group and its MAE and RMSE were 14.31 ms and 23.52 ms, respectively. Comparing the result to the current study for monitoring of gastrointestinal surgery patients, the MAE lies within the obtained error for SR and AF groups.

6.2 HRV parameters error estimation

In Table 3, measurement error of OHR for calculation of linear and non-linear HRV parameters is provided. The variables from right to left are HRV parameter, MAE, MAE (%), RMSE, RMSPE, P05, P95, Bias, Bias (%) and standard deviation. P05 and P95 are 5^{th} and 95^{th} percentiles of the Bias (mean differences), respectively. SD is the standard deviation of biases of all individuals.

Table 3. *The error metrics of HRV parameters in different domains. The error metrics were obtained by taking the average of accepted windows (not the subjects).*

Parameters		MAE	MAE (%)	RMSE	RMSE (%)	P05	P95	Bias	Bias (%)	SD
SDNN	[ms]	2.76	9.11	5.25	14.64	-14.47	2.37	-0.66	1.92	5.42
RMSSD	[ms]	4.28	34.28	5.34	43.23	-1.16	6.07	3.61	32.37	2.21
pNN50	[%]	1.97	139.74	2.81	264.54	-1.40	4.21	0.90	94.92	1.91
NN50	[beats]	5.79	188.75	8.46	332.30	-5.00	14.80	2.27	153.91	6.26
IQR	[ms]	3.58	9.57	6.48	14.02	-19.42	4.35	-0.58	2.31	6.84
Median	[ms]	4.08	0.45	4.76	0.53	-4.00	7.80	0.30	0.03	3.29
Mean RR	[ms]	4.67	0.52	5.97	0.66	-3.53	13.42	0.95	0.10	5.37
Kurtosis	[-]	0.34	10.10	0.60	16.91	-0.47	0.34	0.03	2.84	0.36
Variance	[ms]	238.29	19.86	616.45	45.15	-1449.94	142.35	-126.24	6.95	498.33
Mode	[ms]	13.23	1.47	19.37	2.20	-40.30	34.70	-0.91	-0.07	23.12
HR Mean	[BPM]	0.35	0.51	0.44	0.65	-1.17	0.31	-0.07	-0.10	0.47
TRI	[-]	0.82	11.44	1.08	14.72	-1.76	1.73	0.05	3.41	1.26
TINN	[ms]	0.01	11.08	0.016	15.99	-0.03	0.02	0.0016	4.24	0.01
VLF Abs	[ms^2]	422.38	20.36	631.78	28.48	-1529.24	85.45	-375.94	-17.45	560
LF Abs	[ms^2]	140.18	23.10	203.32	37.17	-467.17	253.71	-9.60	3.75	263.45
HF Abs	[ms^2]	165.37	54.38	222.80	79.74	-264.69	188.59	66.80	43.45	132.54
LF Norm	[n.u.]	7.24	13.71	9.29	18.45	-9.65	5.41	-4.54	-4.77	4.06
HF Norm	[n.u.]	7.24	31.39	9.29	42.66	-5.41	9.65	4.54	26.21	4.06
VLF Log	[log]	0.27	3.6130	0.40	5.38	-0.80	0.05	-0.24	-3.24	0.32
LF Log	[log]	0.22	3.6182	0.32	5.25	-0.60	0.30	-0.018	-0.15	0.31
HF Log	[log]	0.34	6.5297	0.44	8.58	-0.50	0.46	0.21	4.47	0.29
VLF Rel	[%]	7.06	11.97	9.73	15.97	-20.26	-0.50	-6.19	-9.84	6.58
LF Rel	[%]	3.52	22.96	5.19	43.56	-0.75	14.69	1.91	16.46	4.97
HF Rel	[%]	5.38	71.38	7.15	111.91	-2.16	6.62	4.27	67.65	2.63
LF/HF	[n.u.]	0.88	28.70	1.22	36.64	-1.18	0.24	-0.74	-11.79	0.41
ApEn	[-]	0.07	8.21	0.10	12.51	-0.09	0.07	0.02	3.80	0.05
SD_1	[ms]	3.03	34.29	3.77	43.24	-0.82	4.29	2.55	32.37	1.56
SD_2	[ms]	3.48	7.54	7.27	13.20	-21.66	2.42	-2.0023	-1.63	7.73
SD_1/SD_2	[-]	0.10	37.20	0.13	49.42	-0.02	0.13	0.09	35.80	0.04
DFA α_1	[-]	0.14	8.25	0.17	10.31	-0.04	0.18	0.11	6.83	0.07
DFA α_2	[-]	0.08	4.71	0.13	7.42	-0.06	0.16	0.05	3.19	0.09

The error metrics for each HRV parameter is weighted by the number of accepted segments. The RMSE for some parameters is significantly higher than MAE which shows that there is a variance between the individual errors. There is a considerable variance between error metrics of HRV parameters. While the relative mean absolute error for SDNN and HR is 9.57 % and 0.53 %, for parameters such as pNN50 and NN50 it is 139.74 % and 188.75 %, respectively. The reason is that pNN50 and NN50 recorded by the reference device for some subjects were extremely low (close to 0) and the more they get close to 0, the higher values of MAPE is achieved. The accuracy of the OHR device for estimation of HRV parameters can be varied based on patients and parameters.

The results in Table 3 are obtained based on setting the threshold (for accepting segments) to 80% which means that only the segments that the sum of their good quality IBIs were more than 4 minutes have been chosen. Setting the threshold to 80% produces a series of boxplots for different HRV parameters as well as the distribution of the percentage of accepted segments for each individual. The distributions of MAPE are depicted in Figure 8. The bars are clipped at 100% that's why the 75^{th} percentiles for some parameters are not visible in the figure. The left bar is the MAPE, and right bar is the coverage of accepted segments. The bottom part of the bars is 25^{th} percentiles and the upper part of the bars is the 75^{th} percentiles. The dotted circles in the centers of the bars are the median values. Outlier (the most extreme datapoints) have also been determined by red crosses.

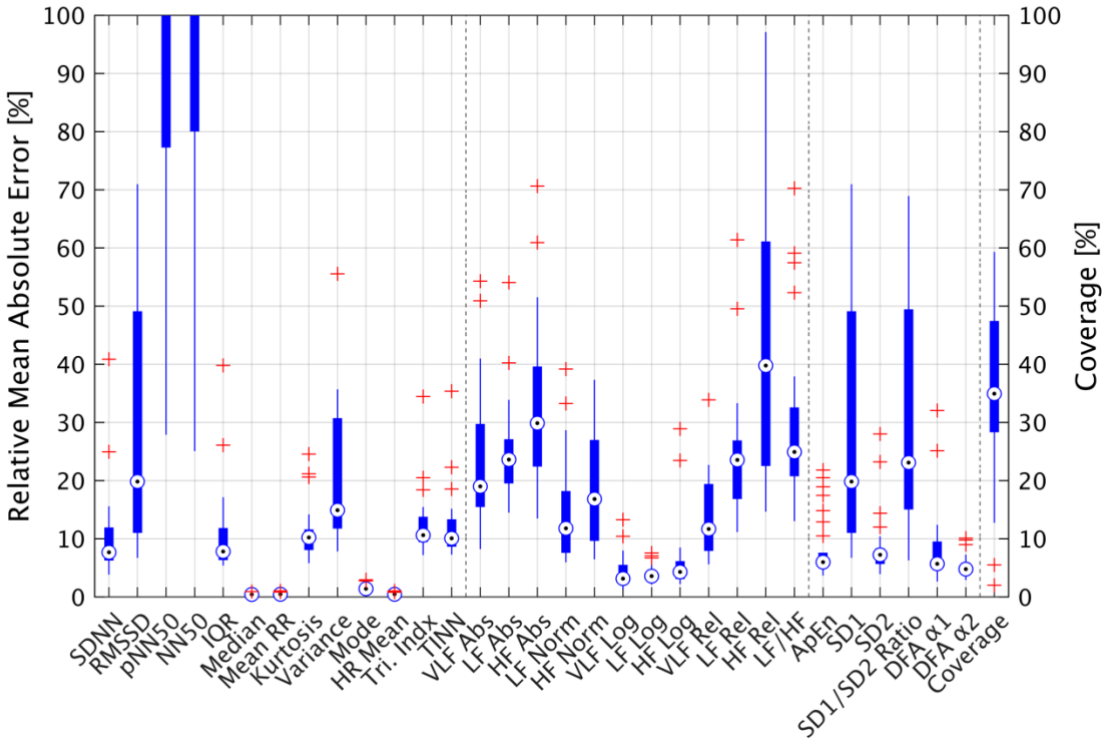

Figure 8. *The distribution of the average MAPE for all the subjects. Each bar contains 30 datapoints which are the number of all subjects. The bar to the right is the coverage of accepted windows after applying the threshold in percentage.*

In Figure 9, the relative bias of all windows of all patients is depicted. It can be concluded that some certain time domain and non-linear parameters such as SDNN and Poincare SD2 have very small biases. On the other hand, RMSSD and Poincare SD1 exhibit higher levels of bias. The reason could be that the irregular and large beat-to-beat intervals can affect RMSSD, pNN50 and SD1 more significantly compared to SDNN and SD2. Concerning the frequency domain HRV parameters, the absolute and relative values of VLF, LF and HF exhibit high bias, however; the same parameters in logarithmic domain have less bias and spreads. The parameters which demonstrate the ratio of frequency and non-linear components such as LF/HF and SD1/SD2 had high systematic underestimation and overestimation, respectively.

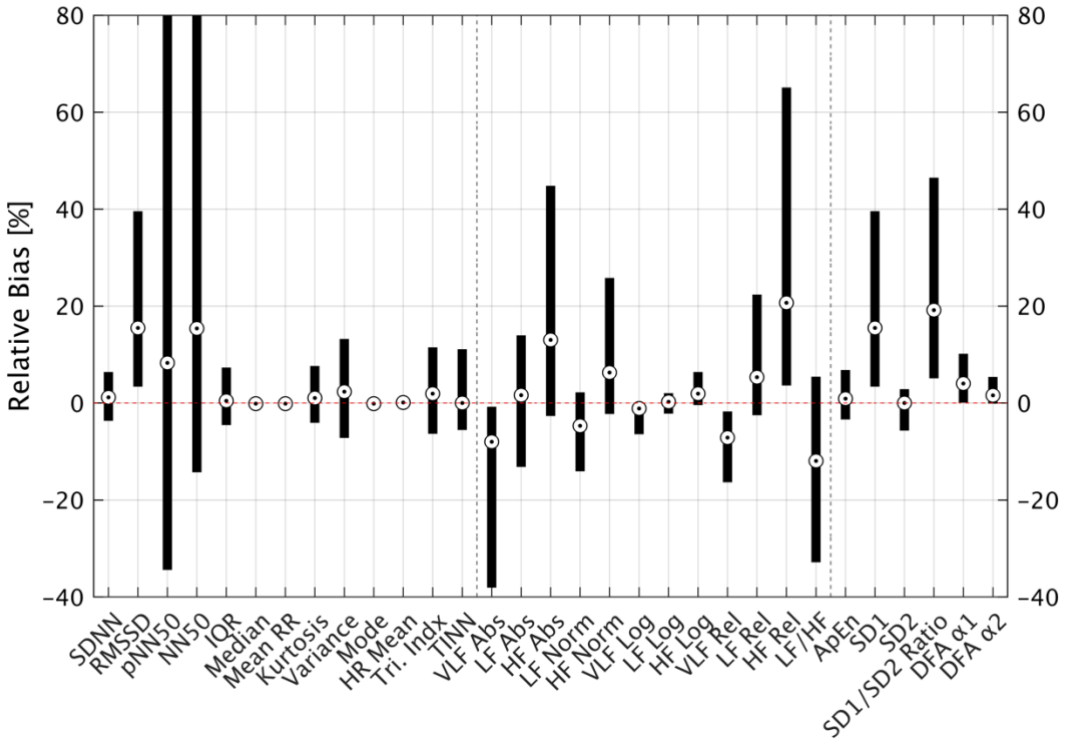

Figure 9. *The analysis of the relative bias for all windows. Each datapoint in each bar represents a segment. The outliers are not depicted in this figure and the lower part of the bar in 25th percentiles and the upper part is the 75th percentile. The circles in the middle of the bars are median values.*

The difference between Table 3 and Figure 8 is that in Table 3, the average of error of all windows was calculated and in Figure 8 it is only the average of relative MAE for individuals. By comparing these two, it can be seen that the average of relative MAE of individuals for some specific parameters is higher than those in Table 3. It can be concluded that the accuracy of OHR is higher for some subjects. For the best 25% of individuals, the relative mean error was around 10% for most of the HRV parameters.

The comparison between the average of windows for each subject for both ECG reference (ground truth) and OHR monitoring (estimation) is illustrated in Figure 10 and 11. In Figure 10 and for pNN50 parameter, it can be seen that the majority of subjects are having a very low HRV values close to 0 which significantly reduced the accuracy of OHR monitoring. For RMSSD in Figure 10 and DFA α_1 in Figure 11, there is a systematic overestimation while for SDNN, the estimation is more accurate as most lines are straight.

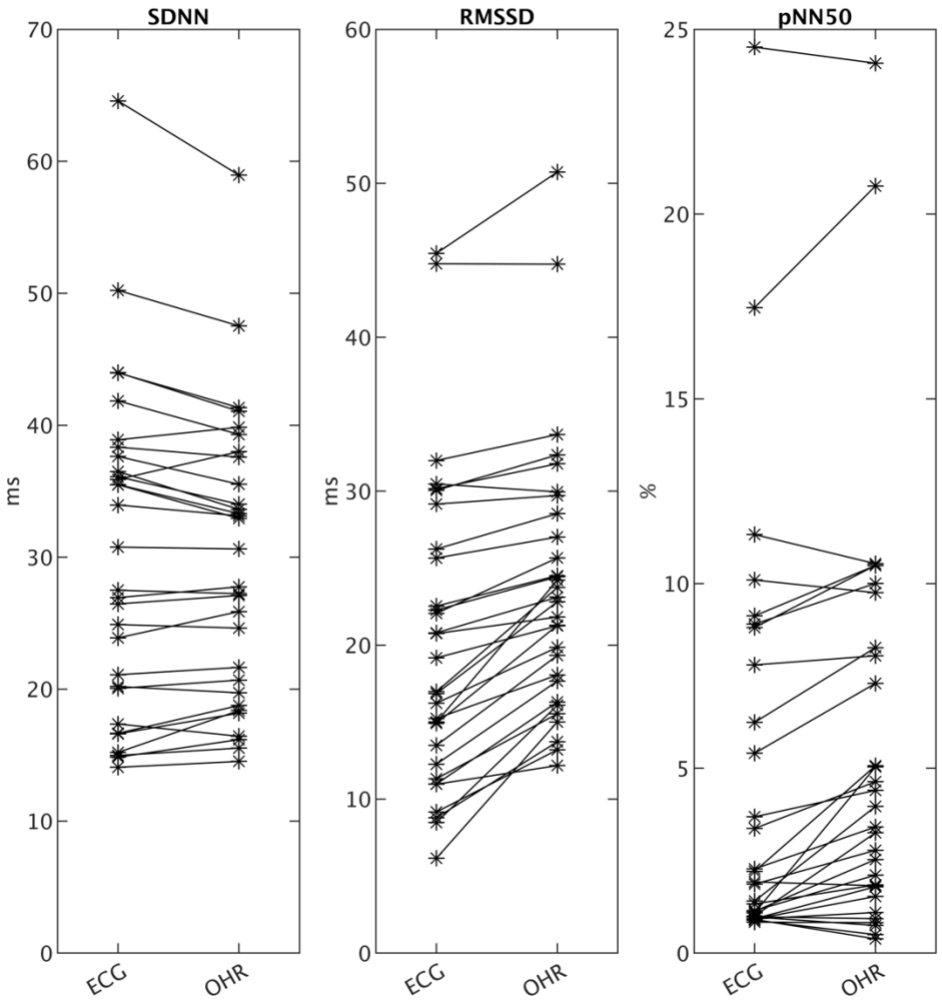

Figure 10. *The comparison between the ECG reference (ground truth) and the OHR device (estimation) for each subject for SDNN, RMSSD and pNN50. There is a systematic overestimation of RMSSD by OHR.*

For the ratio parameters such as LF/HF and SD1/SD2 there are many crossing lines which make them less reliable parameters to be estimated by OHR monitoring. Low levels of HRV in pNN50 ground truth (close to 0) also explains why the values of MAPE in Table 3 and Figure 8 is higher than other parameters.

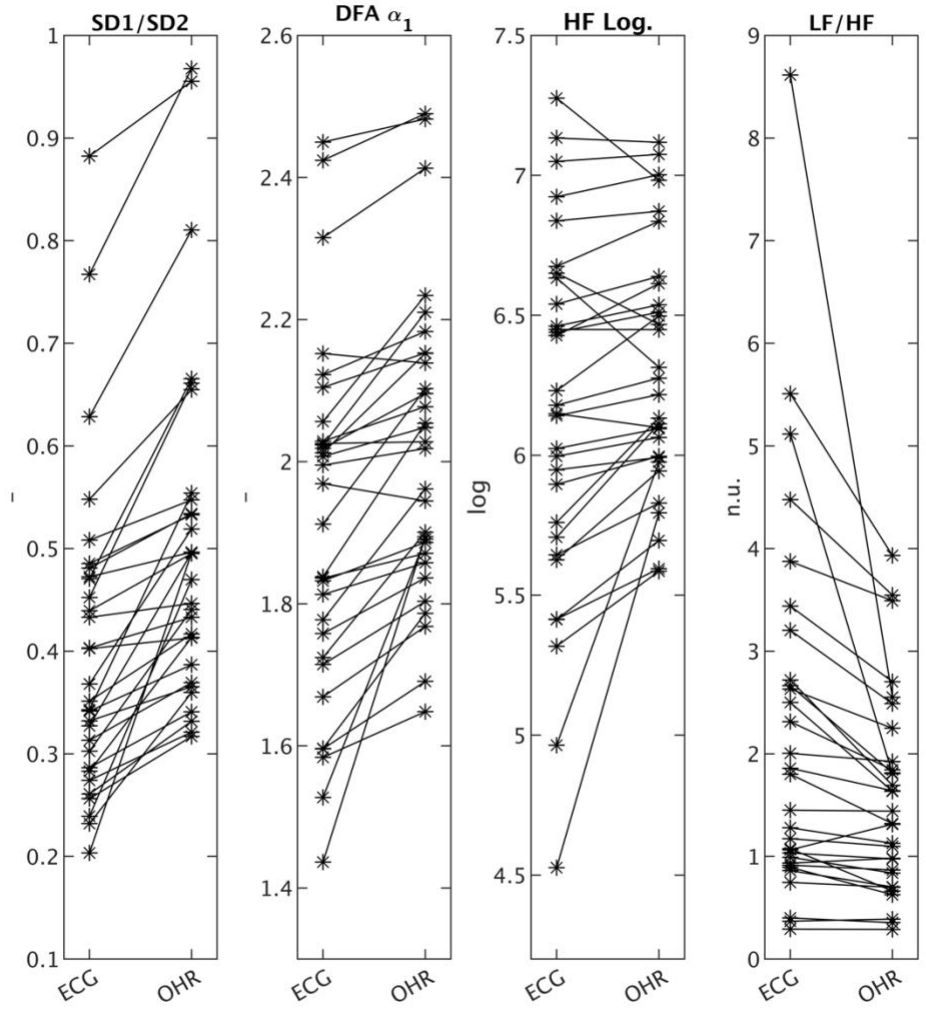

Figure 11. *The comparison of the ground truth and the estimation for SD1/SD2, DFA α_1, HF Log and LF/HF. Each line represents a subject.*

Here in Figure 12, the Bland-Altman plot of SDNN parameter for subjects is depicted. The majority of datapoints which represent the SDNN values of subjects, are placed within the limits of agreements (LoA). The confidence intervals (CI) have been also calculated for LoAs as well as the mean of biases (shaded areas). From statistical point of view, the zero line is placed within the CIs of the bias which shows a high agreement between SDNN values measured by reference and the OHR device [86]. The dashed line in the plot is the best fit line which has a negative trend. It can be concluded that for subjects with higher SDNN values, the OHR device underestimate SDNN.

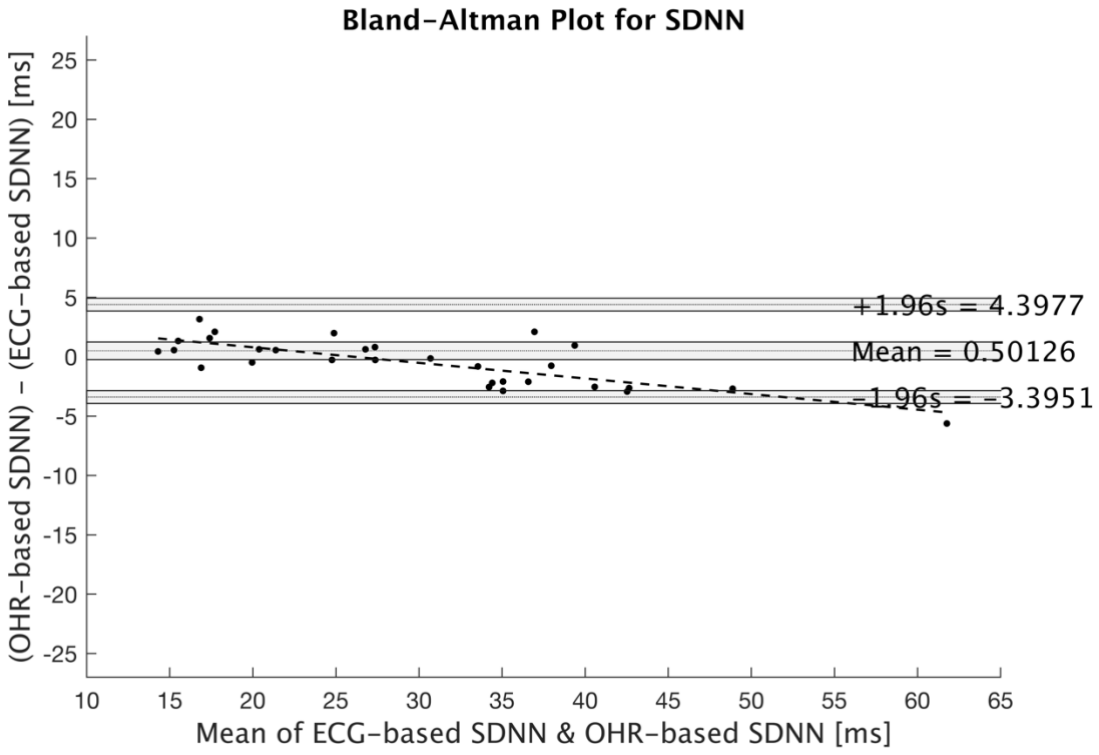

Figure 12. *The Bland-Altman plot the SDNN parameter. The trend of datapoints is negative showing that for higher levels of SDNN, it is overestimated by the OHR. The zero line is placed within the CIs of the bias meaning that the estimation of SDNN is accurate.*

In Figure 13, the Bland-Altman of RMSSD is depicted. In this case, the zero line is not placed within the CIs of the bias which can be a sign that agreement is not as good as SDNN parameter. This was already revealed that RMSSD can be measured less accurately by OHR monitoring compared to SDNN. Similar to the Bland-Altman plot of SDNN, the trend of the best fit line for RMSSD BA plot is negative as well which shows that OHR monitoring starts underestimating RMSSD in higher values of the RMSSD.

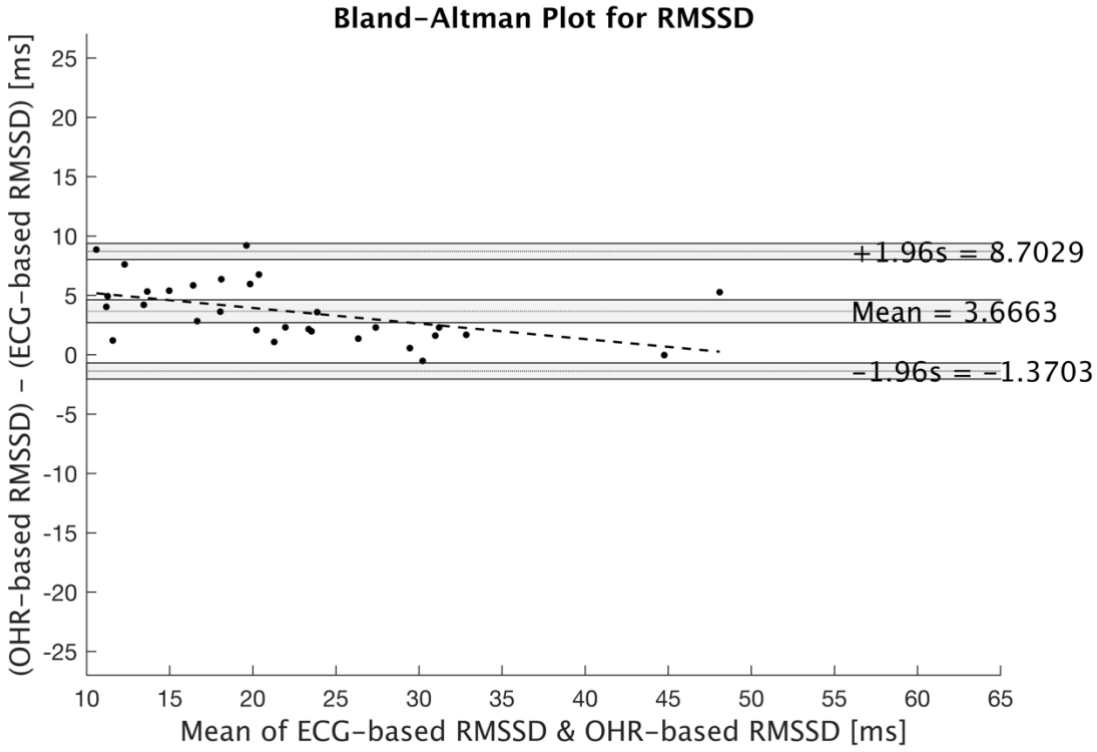

Figure 13. *The Bland-Altman plot for RMSSD parameter. The shaded areas are the CIs of bias and LoAs. The trend of datapoints, similar to SDNN parameter is negative supporting that for higher levels of HRV performance of OHR decreases.*

In Figure 14, the Bland-Altman plot of SDNN but this time for all windows (21315) is depicted. The same results of the BA plot of SDNN of subjects also apply here for the BA plot of windows and the majority of datapoints are placed within the LoAs. The slope of the negative trend in BA plot of SDNN for subjects (Figure 12) is a bit sharper than the slope of the negative trend in BA plot of SDNN for windows (Figure 14) which shows the effect of inaccurate measurements by OHR technology for some individuals. The overestimation of RMSSD for subjects with lower values of HRV happen and as HRV increases, the accuracy of OHR for recording RMSSD also increases.

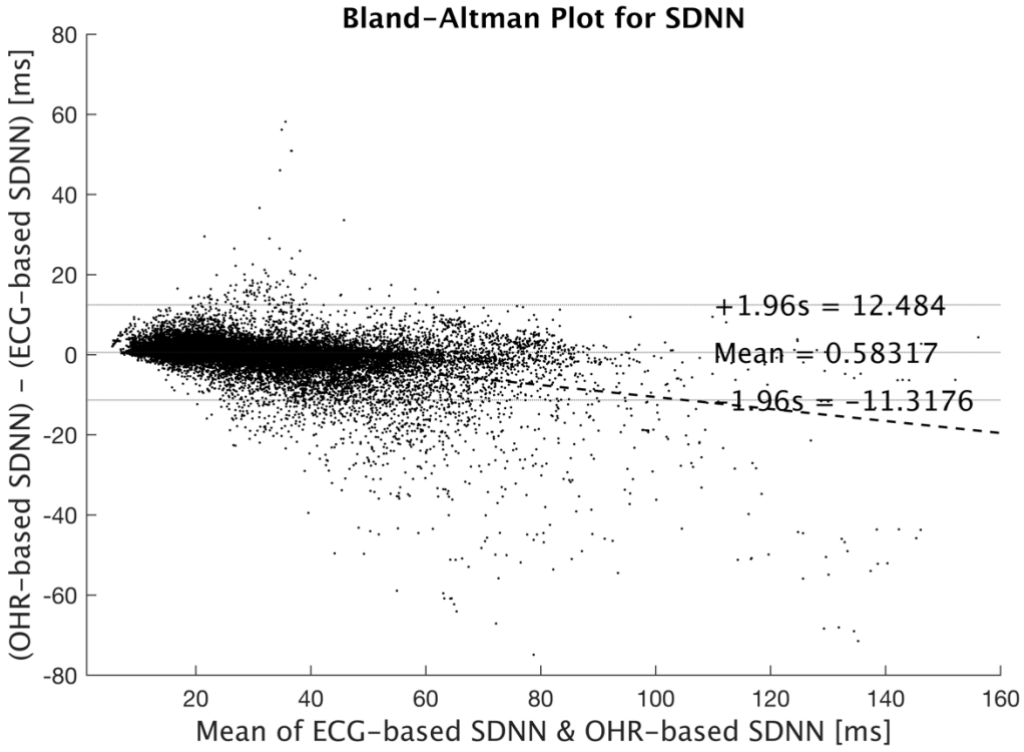

Figure 14. *Bland-Altman plot of SDNN for all windows (21315). Datapoints hold the same trend as BA plot for subjects but with a bit different slope.*

The scatter plot can also provide information regarding the way that two sets of data are related to each other. Unlike Bland-Altman plots, scatter plots do not directly provide information regarding the agreement of the measured data. In Figure 15, the scatter plot of subjects for SDNN parameter is depicted; the dashed line is the best fit line, and the straight line is the equality line (x=y). Datapoints represent the subjects (in total 30 datapoints). The coefficient of determination (r^2) is 0.987 which demonstrate a high relationship between the HRVs for the SDNN parameter.

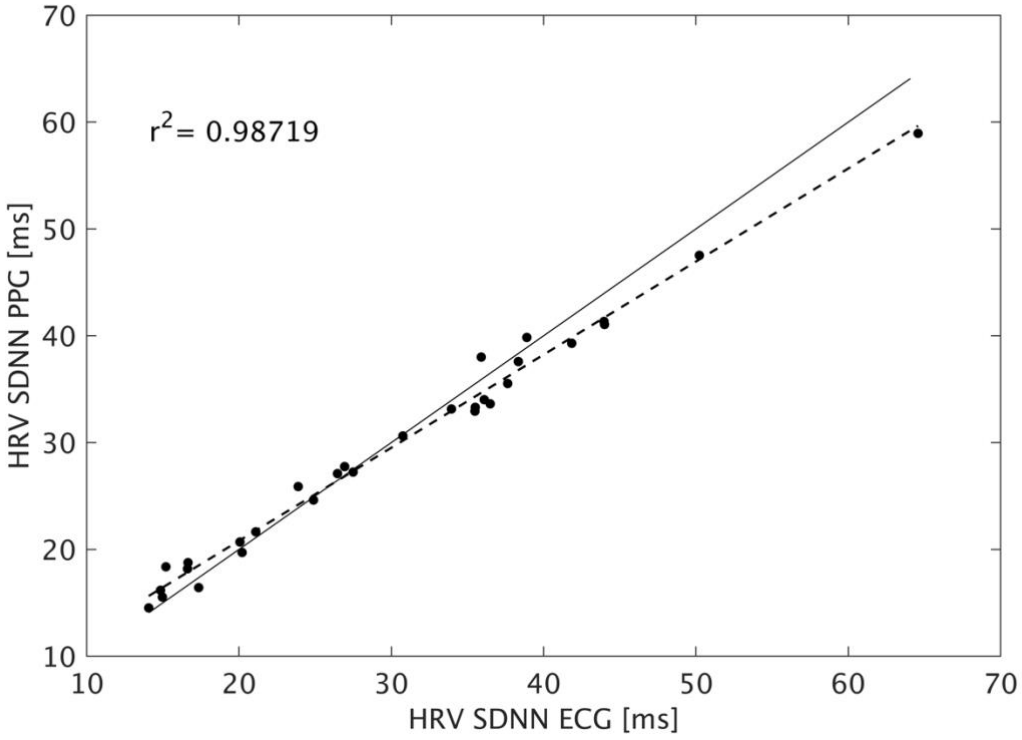

Figure 15. *The scatter plot of SDNN parameter. Each datapoint represent a subject. The dashed line and the straight line are best fit line and the equality line, respectively. The coefficient of determination is 0.987.*

In Figure 16, the scatter plot of RMSSD is depicted. It has also exhibited a high correlation between the two sets of data; however, its coefficient of determination is a bit lower than SDNN's (0.942) and it was already approved that the agreement of the results for SDNN parameter is higher than RMSSD by Bland-Altman plot.

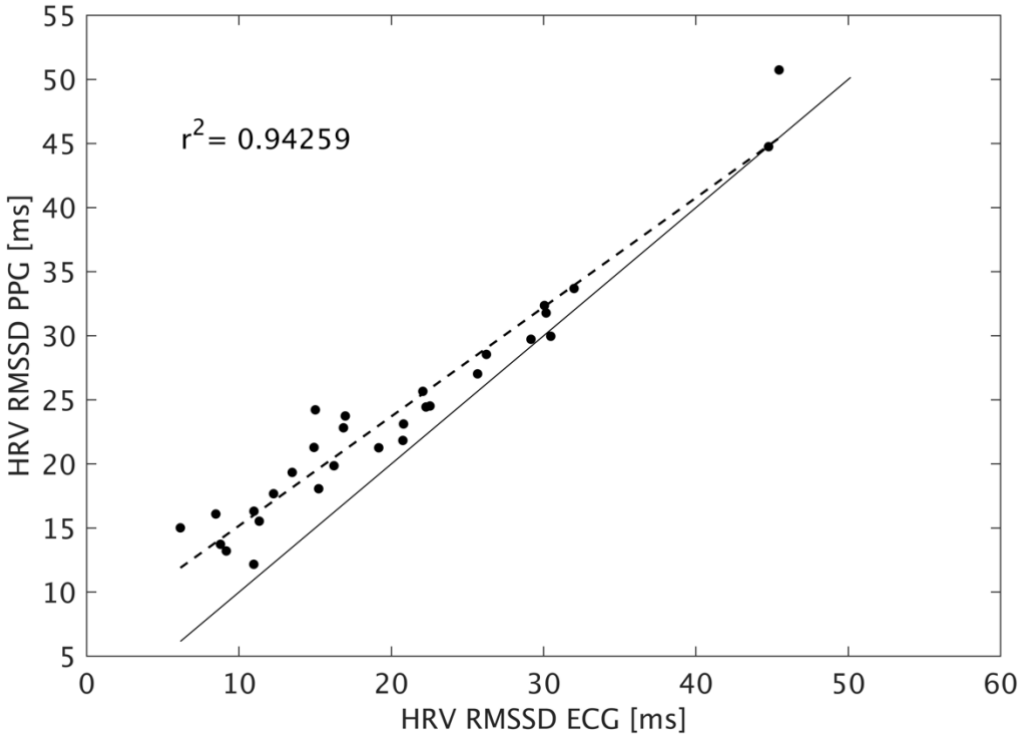

Figure 16. *The cross-correlation plot for RMSSD parameter. The obtained coefficient of determination is 0.942.*

The scatter plot of all 5-minute windows for SDNN parameter is depicted in Figure 17. The coefficient of determination is 0.901 which is lower than the coefficient of determination of SDNN parameter for subjects.

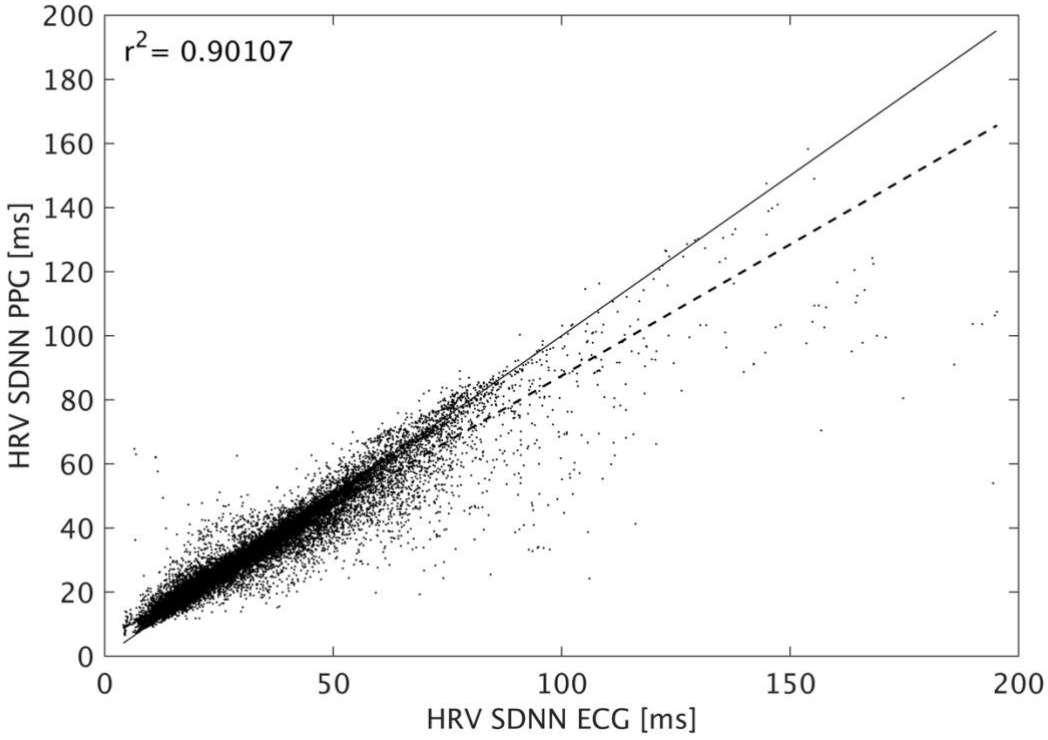

Figure 17. *The cross-correlation plot for all segments of SDNN. Compared to scatter plot of subjects for SDNN, the coefficient of determination decreased to 0.901.*

In Table 4, the coefficient of determination (r^2) of all parameters for all subjects and segments is provided. For most of the HRV parameters, the coefficient of determinations are above 0.8 which shows that two sets of data exhibit an efficient correlation and in general, the coefficient of determinations of subjects are all higher compared to segments.

Table 4. *The coefficient of determination of all parameters for both subjects and segments.*

Parameters	*Coefficient of determination of subjects*	*Coefficient of determination of segments*
SDNN	0.987	0.901
RMSSD	0.942	0.858
pNN50	0.959	0.873
NN50	0.956	0.861
IQR	0.990	0.906
Median	0.999	0.998
Mean RR	0.998	0.997
Kurtosis	0.811	0.494

Variance	0.981	0.779
Mode	0.999	0.971
HR Mean	0.999	0.997
TRI	0.989	0.873
TINN	0.991	0.879
VLF Abs	0.693	0.523
LF Abs	0.941	0.702
HF Abs	0.909	0.763
LF Norm	0.878	0.751
HF Norm	0.878	0.751
VLF Log	0.746	0.565
LF Log	0.926	0.666
HF Log	0.806	0.702
VLF Rel	0.828	0.785
LF Rel	0.922	0.774
HF Rel	0.902	0.800
LF/HF	0.597	0.469
ApEn	0.541	0.353
SD_1	0.942	0.858
SD_2	0.991	0.889
SD_1/SD_2	0.795	0.695
DFA α_1	0.826	0.683
DFA α_2	0.816	0.671

6.3 Effect of ectopic beat removal on accuracy of measurements

The same HRV parameters and error metrics than in Table 2 were again calculated in this section without removing ectopic beats. Figure 18 represents the relative MAE of all HRV parameters with and without applying ectopic beat removal methods. It can be seen that almost all of the error metrics increased significantly due to the existence of ectopic beats. The obtained result emphasizes the importance of ectopic beat removal methods regarding error estimation of HRV parameters by OHR. The details of the result of HRV error estimation are provided in Table 5 of appendix A. Moreover, the MAE of beat-to-beat comparison increased from 10.39 ms to 12.12 ms without removing ectopic beats.

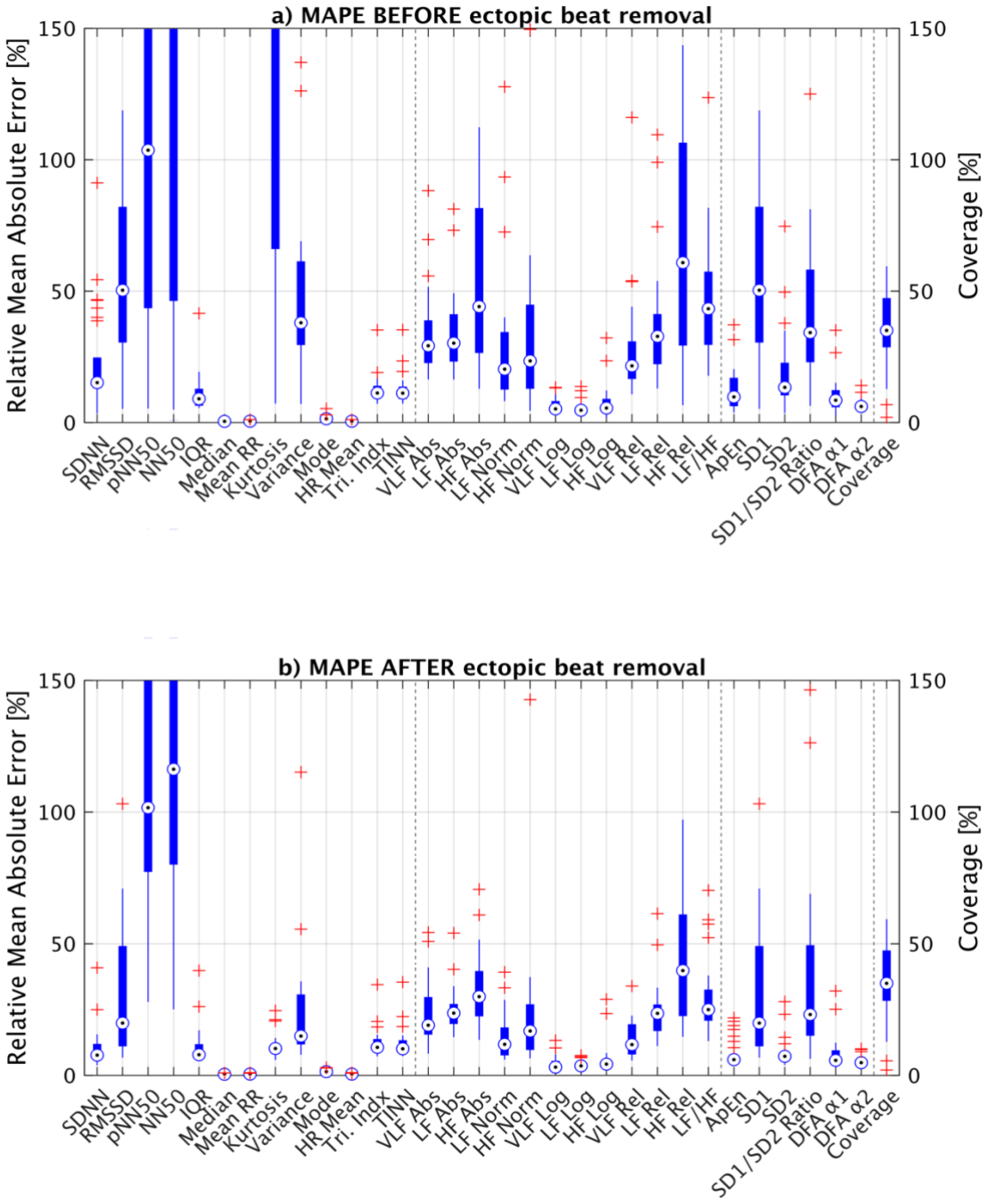

Figure 18. *Effect of ectopic beat removal on MAPE. (a) MAPE before removing ectopic beats. (b) MAPE after removing ectopic beats.*

Summary of the results

In this section, a short summary of the result and discussion regarding the accuracy of the measured HRV parameters is provided.

1. In time domain, measurement of low frequency parameters such as SDNN was done accurately with MAE, relative MAE and percentage bias of 2.76 ms, 9.11 %, and 1.92 %, respectively. RMSSD and pNN50 were estimated less accurately. The relative MAE (34.28 % and 139.74 %) were considerably significant. Mean, median, IQR, kurtosis and mode of IBI intervals were all estimated accurately and the relative MAEs were obtained 0.52 %, 0.45 %, 9.57 %, 10.1 % and 1.47 %, respectively. Triangular index and TINN were also estimated with relatively high accuracy with relative MAE of 11.44 % and 11.08 %, respectively.

2. In frequency domain, the absolute values of frequency parameters were estimated with high errors and the relative MAE of VLF, LF and HF were 20.36 %, 23.1 % and 54.38 %, respectively. However, the frequency parameters in logarithmic domain were estimated with higher accuracy by OHR where the relative MAE for VLF, LF and HF were obtained 3.61 %, 3.618 % and 6.52 %, respectively. The normalized frequency components were estimated with higher error compared to logarithmic values which means that the performance of OHR in the logarithmic domain is the most accurate.

3. For the estimation of non-linear HRV parameters, it was found that ApEn, SD_2, DFA α_1 and DFA α_2 can be estimated with confidence by OHR where the exhibited relative MAE was obtained 8.21 %, 7.54 %, 8.25 % and 4.71 %, respectively. SD_1 was the only non-linear HRV parameter tested, which was estimated with a significantly higher error (relative MAE = 34.29 %) compared to other non-linear HRV parameters and therefore it should be utilized with caution.

4. SD_1/SD_2 and LF/HF were both estimated without efficient accuracy and their relative MAE were 37.2 % and 28.7 %, respectively. Due to having overestimation and underestimation in measurements they still need further improvements to be used confidently.

Several studies have evaluated the HRV parameters of patients in different conditions, such as before and after the surgeries or for the patients who had complications after the surgery and the ones who did not have any. In a study by Ernst et al [90], subjects were undergone hip surgeries and it was seen that complications after surgery were decreasing the HRV parameters such as RMSSD and frequency domain parameters of HRV. For RMSSD parameter, the mean value together with standard deviation was 18.2 $\pm$ 0.9 ms for the "uncomplicated" group and the for the "complicated" group it was 14.9 $\pm$ 1.3. Based on the result in the present study, MAE for RMSSD was 4.28 ms and RMSE was 5.34 ms which means that the OHR device cannot efficiently distinguish these two groups of subjects for RMSSD and frequency domain HRV parameters. The calculation of frequency domain HRV parameters in the present study was done based on single 5-minute segments and combining more segments could possibly improve the results.

In another study by Ushiyama et al [91], SDNN was calculated for the complicated and uncomplicated groups. For the "complicated group", SDNN was 48.7 ± 24.4 (mean ± standard deviation) and for the "uncomplicated group" it was 71.2 ± 19.6. In the present study, the MAE and RMSE of SDNN were 2.76 ms and 5.25 ms indicating that these two groups can be clearly distinguished by OHR technology.

6.4 Limitations and future work

Some of the limitation of the study together with some suggestions for the future studies are provided in this section.

- Proper BBIs alignment minimizes the final beat-to-beat error. If the signals are aligned properly and false beats are removed efficiently, the final beat-to-beat error will be the lowest possible. For some subjects, the signals went out of sync for long-term recordings due to the time drift caused by different internal clocks. It was therefore required to align the signals multiple times which could be prone to miscalculations, so more signal processing methods and algorithms for automatic synchronization can be investigated.

- The accuracy of the OHR monitoring is very dependent on the motion artifacts and ambient light. By comparing the ECG RRIs and PPG IBIs it could clearly be seen that during daytime the accuracy of estimation by OHR device reduces significantly.

The main reason is the movements by the patients. It is therefore required to conduct more tests to evaluate the effect of ambient light on the accuracy of estimation and possibly investigating the methods to minimize the negative effects of ambient light and motion artifacts.

- The subjects of the present study were all sharing almost similar skin pigmentation based on Fitzpatrick skin types and the accuracy of the OHR estimation can be different depending on the skin pigmentation. So, it would be beneficial to evaluate the accuracy of OHR for darker skins. Moreover, the green light was utilized as the source (LED) for this study and the effects of other wavelengths on the accuracy of measurements could be further investigated.

7. CONCLUSION

Continuous monitoring of post-surgery patients could provide information about complications after surgeries and OHR is one comfortable option for monitoring of surgery patients. The aim of this thesis was to evaluate the accuracy of OHR technology for post-operative patient monitoring (by measuring beat-to-beat error and HRV parameter error). It was revealed that OHR can produce accurate beat-to-beat information. The accuracy of OHR was further investigated by estimating HRV parameters in time and frequency domain as well as non-linear parameters and error metrics were calculated. It was concluded that the accuracy of estimation was not the same for all HRV parameters. While the final error metrics were relatively low for time domain parameters such as SDNN, OHR was overestimating parameters such as RMSSD, and for pNN50/NN50, the estimation was done less accurately by the OHR. In frequency domain, the absolute values of parameters were estimated less accurately, however, after converting them to logarithmic domain, error metrics were reduced significantly. Among non-linear parameters, except for SD_1, the rest of the investigated parameters were having a relatively low error. It was also concluded that the preprocessing the IBIs and cleaning up the ectopic beats can significantly improve the accuracy of estimation.

Finally, the OHR technology can be a comfortable alternative for the conventional ECG recordings due to the benefits that it provides for the users and the healthcare personnel. However, based on the findings in this thesis, there is still room for improvement in estimating HRV parameters by investigating more robust approaches of IBIs estimation which are less prone to be affected by artifacts.

REFERENCES

[1] S. Park and S. Jayarman, "Enhancing the Quality of Life Through Wearable Technology," *IEEE Engineering in Medicine and Biology Magazine,* vol. 22, pp. 41-48, May-June 2003.

[2] "The Top 10 Causes of Death," 9 December 2020. [Online]. Available: https://www.who.int/news-room/fact-sheets/detail/the-top-10-causes-of-death.

[3] G. Silveri, M. Merlo, L. Restivo, B. De Paola, A. Miladinović, M. Ajčević, G. Sinagra and A. Accardo, "Identification of Ischemic Heart Disease by Using Machine Learning Technique Based on Parameters Measuring Heart Rate Variability".

[4] I. Goldenberg, R. Goldkorn, N. Shlomo, M. Einhorn, J. Levitan, R. Kuperstein, R. Klempfner and B. Johnson, "Heart Rate Variability for Risk Assessment of Myocardial Ischemia in Patients Without Known Coronary Artery Disease: The HRV-DETECT (Heart Rate Variability for the Detection of Myocardial Ischemia) Study," *American Heart Association.*

[5] A. J. Burger, M. Charlamb and H. B. Sherman, "Circadian Patterns of Heart Rate Variability in Normals, Chronic Stable Angina and Diabetes Mellitus," *International Journal of Cardiology,* pp. 41-48, 1999.

[6] A. Voss, S. Schulz, R. Schroeder, M. Baumert and P. Caminal, "Methods Derived from Nonlinear Dynamics for Analysing Heart Rate Variability," *Philosophical Transactions of the Royal Society of London,* 2009.

[7] H. V. Huikuri, A. Castellanos and R. J. Myerburg, "Sudden Death Due to Cardiac Arrhythmias," *The New England journal of medicine,* pp. 1473-1482, 15 11 2001.

[8] C. Park, P. H. Chou, Y. Bai, R. Matthews and A. Hibbs, "An Ultra-Wearable, Wireless, Low Power ECG Monitoring System," *2006 IEEE Biomedical Circuits and Systems Conference,* 2006.

[9] C. Saritha, V. Sukanya and Y. N. Murthy, "ECG Signal Analysis Using Wavelet Transforms," *Bulg. J. Phys,* pp. 68-77, 2008.

[10] D. Podvyaznikov, "Medium," 22 November 2017. [Online]. Available: https://medium.com/data-analysis-center/annotating-ecg-signals-with-hidden-markov-model-56f8b9abd83a. [Accessed 28 June 2021].

[11] J. Crawford and L. Doherty, Practical aspects of ECG recording, Cumbria England : M&K Update, 2012.

[12] B.-U. Kohler, C. Hennig and R. Orglmeister, "The Principles of Software QRS Detection," *IEEE engineering in medicine and biology magazine,* pp. 42-57, 2002.

[13] M. L. Ahlstrom and W. J. Tompkins, "Automated High-Speed Analysis of Holter Tapes with Microcomputers," *IEEE transactions on biomedical engineering,* pp. 651-657, 1983.

[14] L. Keselbrener, M. Keselbrener and S. Akselrod, "Nonlinear High Pass Filter for R-wave Detection in ECG Signal," *Medical engineering & physics,* pp. 481-484, 1997.

[15] J. Leski and E. Tkacz, "A new Parallel Concept for QRS Complex Detector," *1992 14th Annual International Conference of the IEEE Engineering in Medicine and Biology Society,* pp. 555-556, 1992.

[16] S. Suppappola and Y. Sun, "Nonlinear Transforms of ECG Signals for Digital QRS Detection: A Quantitative Analysis," *IEEE transactions on biomedical engineering,* pp. 397-400, 1994.

[17] M. Bahoura, M. Hassani and M. Hubin, "DSP Implementation of Wavelet Transform for Real Time ECG Wave Forms Detection and Heart Rate Analysis," *Computer methods and programs in biomedicine,* pp. 35-44, 1997.

[18] S. Kadambe, R. Murray and G. Boudreaux-Bartels, "Wavelet Transform-Based QRS Complex Detector," *IEEE transactions on biomedical engineering,* pp. 838-848, 1999.

[19] C. Li, C. Zheng and C. Tai, "Detection of ECG Characteristic Points Using Wavelet Transforms," *IEEE transactions on biomedical engineering,* pp. 21-28, 1995.

[20] Q. Xue, Y. Hu and W. Tompkins, "Neural-Network-Based Adaptive Matched Filtering for QRS Detection," *IEEE transactions on biomedical engineering,* pp. 317-329, 1992.

[21] Z. Dokur, T. Ölmez, E. Yazgan and O. K. Ersoy, "Detection of ECG Waveforms by Neural Networks," *Medical engineering & physics,* pp. 738-741, 1997.

[22] J. Mateo and P. Laguna, "Analysis of heart rate variability in the presence of ectopic beats using the heart timing signal," *IEEE transactions on biomedical engineering,* pp. 334-343, 2003.

[23] M. A. Salo, H. V. Huikuri and T. Seppanen, "Ectopic Beats in Heart Rate Variability Analysis: Effects of Editing on Time and Frequency Domain Measures," *Annals of noninvasive electrocardiology,* pp. 5-17, 2001.

[24] C. Levkov, G. Mihov, R. Ivanov, I. Daskalov, I. Christov and I. Dotsinsky, "Removal of power-line interference from the ECG: a review of the subtraction procedure," *Biomedical engineering online,* pp. 50-50, 2005.

[25] R. Jane, P. Laguna, N. Thakor and P. Caminal, "Adaptive baseline wander removal in the ECG: Comparative analysis with cubic spline technique," *Proceedings Computers in Cardiology,* pp. 143-146, 1992.

[26] M. Mneimneh, E. Yaz, M. Johnson and R. Povinelli, "An adaptive kalman filter for removing baseline wandering in ECG signals," in *2006 Computers in Cardiology*, 2006.

[27] X. Lisheng, W. Kuanquan, D. Zhang and S. Cheng, "Adaptive baseline wander removal in the pulse waveform," *Proceedings of 15th IEEE Symposium on Computer-Based Medical Systems (CBMS 2002),* pp. 143-148, 2002.

[28] P. Langley, J. Dark and A. Murray, "QT dispersion analysis of a transplant assessment group," in *Computers in Cardiology 2000. Vol.27 (Cat. 00CH37163)*, 2000.

[29] P. Mithun, P. C. Pandey, T. Sebastian, P. Mishra and V. K. Pandey, "A wavelet based technique for suppression of EMG noise and motion artifact in ambulatory ECG," *2011 Annual International Conference of the IEEE Engineering in Medicine and Biology Society,* pp. 7087-7090, 2011.

[30] G. Bortolan and I. Christov, "Dynamic filtration of high-frequency noise in ECG signal," in *Computing in Cardiology 2014*, 2014.

[31] F. Bagheri, N. Ghafarnia and F. Bahrami, "Electrocardiogram (ECG) Signal Modeling and Noise Reduction Using Hopfield Neural Networks," *Engineering, technology & applied science research,* pp. 345-348, 2013.

[32] A. Savitzky and M. J. E. Golay, "Smoothing and Differentiation of Data by Simplified Least Squares Procedures," *Analytical chemistry (Washington),* pp. 1627-1639, 1964.

[33] P. Lander and E. Berbari, "Time-frequency plane Wiener filtering of the high-resolution ECG: development and application," *IEEE transactions on biomedical engineering,* pp. 256-265, 1997.

[34] J. Paul, M. Reddy and V. Kumar, "A transform domain SVD filter for suppression of muscle noise artefacts in exercise ECG's," *IEEE transactions on biomedical engineering,* pp. 654-663, 2000.

[35] A. Puranen, T. Halkola, O. Kirkeby and A. Vehkaoja, "Effect of skin tone and activity on the performance of wrist-worn optical beat-to-beat heart rate monitoring," 2020.

[36] Y. Maeda, M. Sekine, T. Tamura, A. Moriya, T. Suzuki and K. Kameyama, "Comparison of reflected green light and infrared photoplethysmography," *Annual International Conference of the IEEE Engineering in Medicine and Biology Society,* pp. 2270-2272, 2008.

[37] P. Renevey, J. Sola, P. Theurillat, M. Bertschi, J. Krauss, D. Andries and C. Sartori, "Validation of a wrist monitor for accurate estimation of RR intervals during sleep," *Annual International Conference of the IEEE Engineering in Medicine and Biology Society (EMBC),* pp. 5493-5496, 2013.

[38] B. Jönsson, C. Laurent, T. Skau and L.-G. Lindberg, "A New Probe for Ankle Systolic Pressure Measurement Using Photoplethysmography (PPG)," *Annals of biomedical engineering,* pp. 232-239, 2005.

[39] K. H. SHELLEY, D. TAMAI, D. JABLONKA, M. GESQUIERE, R. G. STOUT and D. G. SILVERMAN, "The effect of venous pulsation on the forehead pulse oximeter wave form as a possible source of error in spo2 calculation," *Anesthesia and analgesia,* pp. 743-747, 2005.

[40] Y. Maeda, M. Sekine, T. S. J. Tamura, N. Smalheiser, H. Andrade, J. Suri, A. Emrouznejad, A. Emrouznejad, P. Dey, N. Smalheiser, R. Shi, R. Achara U, R. Achara U and R. Shi, "Relationship Between Measurement Site and Motion Artifacts in Wearable Reflected Photoplethysmography," *Journal of medical systems,* pp. 969-976, 2011.

[41] L. Nilsson, T. Goscinski, S. Kalman, L.-G. Lindberg and A. Johansson, "Combined photoplethysmographic monitoring of respiration rate and pulse: a comparison between different measurement sites in spontaneously breathing subjects," *Acta anaesthesiologica Scandinavica,* pp. 1250-1257, 2007.

[42] V. Hartmann, H. Liu, F. Chen, Q. Qiu, S. Hughes and D. Zheng, "Quantitative Comparison of Photoplethysmographic Waveform Characteristics: Effect of Measurement Site," *Frontiers in physiology,* pp. 198-198, 2019.

[43] Y. Mendelson and B. Ochs, "Noninvasive pulse oximetry utilizing skin reflectance photoplethysmography," *IEEE transactions on biomedical engineering,* pp. 798-805, 1988.

[44] M. Lemay, M. Bertschi, J. Sola, P. Renevey, J. Parak and I. Korhonen, "Application of Optical Heart Rate Monitoring," in *Wearable Sensors*, Elsevier Inc, 2015, pp. 105-129.

[45] F.-H. Huang, P.-J. Yuan, K.-P. Lin, H.-H. Chang and C.-L. Tsai, "Analysis of Reflectance Photoplethysmograph Sensors," 2011.

[46] R. Mccraty and F. Shaffer, "Heart Rate Variability: New Perspectives on Physiological Mechanisms, Assessment of Self-regulatory Capacity, and Health Risk," *Global Advances in Health and Medicine,* pp. 46-61, 2015.

[47] T. A. J. MCEWEN and A. A. F. SIMA, "Autonomic neuropathy in BB rat: assessment by improved method for measuring heart-rate variability," *Diabetes (New York, N.Y.),* pp. 251-255, 1987.

[48] F. Shaffer and J. P. Ginsberg, "An Overview of Heart Rate Variability Metrics and Norms," *Frontiers in public health,* pp. 258-258, 2017.

[49] "Garmin," [Online]. Available: https://support.garmin.com/en-US/?faq=04pnPSBTYSAYL9FylZoUl5. [Accessed 29 June 2021].

[50] U. Rajendra Acharya, K. Paul Joseph, N. Kannathal, C. M. Lim and J. S. Suri, "Heart rate variability: a review," *Medical & biological engineering & computing,* pp. 1031-1051, 2006.

[51] "Heart rate variability : standards of measurement, physiological interpretation, and clinical use," *Electrophysiology, Task Force of the European Society,* pp. 1043-1065, 1996.

[52] M. Hadase, A. Azuma, K. Zen, S. Asada, T. Kawasaki, T. Kamitani, S. Kawasaki, H. Sugihara and H. Matsubara, "Very low frequency power of heart rate variability is a powerful predictor of clinical prognosis in patients with congestive heart failure," *Circulation journal : official journal of the Japanese Circulation Society,* pp. 343-347, 2004.

[53] F. Shaffer, R. McCraty and C. L. Zerr, "A healthy heart is not a metronome: an integrative review of the heart's anatomy and heart rate variability," *Frontiers in psychology,* pp. 1040-1040, 2014.

[54] D. J. Ewing, J. M. Neilson and P. Travis, "New method for assessing cardiac parasympathetic activity using 24 hour electrocardiograms," *British Heart Journal,* pp. 396-402, 1984.

[55] J. E. Mietus, C.-K. Peng, I. Henry, R. L. Goldsmith and A. L. Goldberger, "The pNNx files: re-examining a widely used heart rate variability measure," *Heart (British Cardiac Society),* pp. 378-380, 2002.

[56] J. Bigger, R. E. Kleiger, J. L. Fleiss, L. M. Rolnitzky, R. C. Steinman and J. Miller, "Components of heart rate variability measured during healing of acute myocardial infarction," *The American journal of cardiology,* pp. 208-215, 1988.

[57] S. Chakko, R. F. Mulingtapang, H. V. Huikuri, K. M. Kessler, B. J. Materson and R. J. Myerburg, "Alterations in heart rate variability and its circadian rhythm in hypertensive patients with left ventricular hypertrophy free of coronary artery disease," *The American heart journal,* pp. 1364-1372, 1993.

[58] B. M. Szabó, D. J. van Veldhuisen, N. van der Veer, J. Brouwer, P. A. De Graeff and H. J. Crijns, "Prognostic Value of Heart Rate Variability in Chronic Congestive Heart Failure Secondary to Idiopathic or Ischemic Dilated Cardiomyopathy," *The American journal of cardiology,* pp. 978-980, 1997.

[59] H. Tsuji, M. G. Larson, J. F. J. Venditti, E. S. Manders, J. C. Evans, C. L. Feldman and D. Levy, "Impact of reduced heart rate variability on risk for cardiac events. The Framingham Heart Study," *Circulation (New York, N.Y.),* pp. 2850-2855, 1996.

[60] G. Zuanetti, J. M. Neilson, R. Latini, E. Santoro, A. P. Maggioni and D. J. Ewing, "Prognostic significance of heart rate variability in post-myocardial infarction patients in the fibrinolytic era : The GISSI-2 results," *Circulation (New York, N.Y.),* pp. 432-436, 1996.

[61] J. Taelman, S. Vandeput, A. Spaepen and S. Van Huffel, "Influence of Mental Stress on Heart Rate and Heart Rate Variability," in *4th European Conference of the International Federation for Medical and Biological Engineering*, 2009.

[62] D. Malaspina, G. Bruder, G. W. Dalack, S. Storer, M. Van Kammen, X. Amador, A. Glassman and J. Gorman, "Diminished cardiac vagal tone in schizophrenia: Associations to brain laterality and age of onset," *Biological psychiatry (1969),* pp. 612-617, 1997.

[63] J. H. Lee, I. Y. Huh, J. M. Lee, H. K. Lee, I. S. Han and H. J. Kang, "Relation of Various Parameters Used to Estimate Cardiac Vagal Activity and Validity of pNN50 in Anesthetized Humans," *Kosin Medical Journal (Online),* pp. 369-379, 2018.

[64] N. Natarajan, A. K. Balakrishnan and K. Ukkirapandian, "A study on analysis of Heart Rate Variability in hypertensive individuals," *International journal of biomedical and advance research,* p. 109, 2014.

[65] J. Koenig, M. N. Jarczok, M. Warth, R. J. Ellis, C. Bach, T. K. Hillecke and J. F. Thayer, "Body mass index is related to autonomic nervous system activity as measured by heart rate variability — A replication using short term measurements," *The Journal of nutrition, health & aging,* pp. 300-302, 2014.

[66] M. S. Silvetti, F. Drago and P. Ragonese, "Heart rate variability in healthy children and adolescents is partially related to age and gender," *International journal of cardiology,* pp. 169-174, 2001.

[67] E. Buccelletti, E. Gilardi, E. Scaini, L. Galiuto, R. Persiani, A. Biondi, F. Basile and N. G. Silveri, "Heart rate variability and myocardial infarction: systematic literature review

and metanalysis," *European review for medical and pharmacological sciences,* p. 299, 2009.

[68] A. Reyners, B. Hazenberg, W. Reitsma and A. Smit, "Heart rate variability as a predictor of mortality in patients with AA and AL amyloidosis," *European heart journal,* pp. 157-161, 2002.

[69] Y. Guo, J. Palmer, F. Strasser, S. Yusuf and E. Bruera, "Heart rate variability as a measure of autonomic dysfunction in men with advanced cancer," *European journal of cancer care,* pp. 612-616, 2013.

[70] C. M. M. Licht, E. J. C. de Geus, R. van Dyck and B. W. J. H. Penninx, "Association between Anxiety Disorders and Heart Rate Variability in The Netherlands Study of Depression and Anxiety (NESDA)," *Psychosomatic medicine,* pp. 508-518, 2009.

[71] N. Lakusic, D. Mahovic, P. Kruzliak, J. Cerkez Habek, M. Novak and D. S. M. S. Cerovec, "Changes in Heart Rate Variability after Coronary Artery Bypass Grafting and Clinical Importance of These Findings," *BioMed research international,* 2015.

[72] J. P. Singh, M. G. Larson, C. J. O'Donnell, P. F. Wilson, H. Tsuji, D. M. Lloyd-Jones and D. Levy, "Association of hyperglycemia with reduced heart rate variability (The Framingham Heart Study)," *The American journal of cardiology,* pp. 309-312, 2000.

[73] C. M. DeGiorgio, P. Miller, S. Meymandi, A. Chin, J. Epps, S. Gordon, J. Gornbein and R. M. Harper, "RMSSD, a measure of vagus-mediated heart rate variability, is associated with risk factors for SUDEP: The SUDEP-7 Inventory," *Epilepsy & behavior,* pp. 78-81, 2010.

[74] N. Risdiana, "Comparison of Root Mean Square of Successive Differences (RMSSD) Among Adolescent Smokers and Nonsmokers in Yogyakarta," *Advanced science letters,* pp. 12660-12664, 2017.

[75] S. L. Birch, M. J. Duncan and C. Franklin, "Overweight and reduced heart rate variability in British children: An exploratory study," *Preventive medicine,* pp. 430-432, 2012.

[76] M. Brennan, M. Palaniswami and P. Kamen, "Do existing measures of Poincare plot geometry reflect nonlinear features of heart rate variability?," *IEEE transactions on biomedical engineering,* pp. 1342-1347, 2001.

[77] M. Brennan, M. Palaniswami and P. Kamen, "Poincaré plot interpretation using a physiological model of HRV based on a network of oscillators," *American Journal of Physiology - Heart and Circulatory Physiology,* pp. 1873-1886, 2002.

[78] L. Mourot, M. Bouhaddi, S. Perrey, J.-D. Rouillon and J. Regnard, "Quantitative Poincaré plot analysis of heart rate variability: effect of endurance training," *European journal of applied physiology,* pp. 79-87, 2004.

[79] "kubios.com," [Online]. Available: https://www.kubios.com/hrv-analysis-methods/#Taskforce1996. [Accessed 29 June 2021].

[80] M. Malik, "Heart rate variability : standards of measurement, physiological interpretation, and clinical use," *Electrophysiology, Task Force of the European Society,* pp. 1043-1065, 1996.

[81] P. Scheffler, S. Muccio, G. Egiziano, R. J. Doonan, A. Yu, F. Carli and S. S. Daskalopoulou, "Heart Rate Variability Exhibits Complication-Dependent Changes Postsurgery," *Angiology,* pp. 597-603, 2013.

[82] G. Ernst, L. O. Watne, F. Frihagen, T. B. Wyller, A. Dominik and M. T. E. Rostrup, "Decreases in heart rate variability are associated with postoperative complications in hip fracture patients," *PloS one,* Vols. e0180423-e0180423, 2017.

[83] L. Claudia, I. Oscar, P.-G. Héctor and V. J. Marco, "Poincare plot indexes of heart rate variability capture dynamic adaptations after haemodialysis in chronic renal failure patients," *Clinical physiology and functional imaging,* pp. 72-80, 2003.

[84] C. Hoog Antink, Y. Mai, M. Peltokangas, S. Leonhardt, N. Oksala and A. Vehkaoja, "Accuracy of heart rate variability estimated with reflective wrist-PPG in elderly vascular patients," *Scientific reports,* vol. 11, pp. 8123-8123, 2021.

[85] J. Pan and W. J. Tompkins, "A Real-Time QRS Detection Algorithm," *IEEE transactions on biomedical engineering,* pp. 230-236, 1985.

[86] S. Saalasti, M. Seppänen and A. Kuusela, "Artefact Correction For Heart Beat Interval Data," *Advanced Methods for Processing Bioelectrical Signals,* 2004.

[87] R. Thuraisingham, "Preprocessing RR interval time series for heart rate variability analysis and estimates of standard deviation of RR intervals," *Computer methods and programs in biomedicine,* pp. 78-82, 2006.

[88] D. Giavarina, "Understanding Bland Altman analysis," *Biochemia medica,* pp. 141-151, 2015.

[89] S. Haghayegh, H.-A. Kang, S. Khoshnevis, M. H. Smolensky and K. R. Diller, "A comprehensive guideline for Bland-Altman and intra class correlation calculations to properly compare two methods of measurement and interpret findings," *Physiological measurement,* pp. 055012-055012, 2020.

[90] J. Parak, A. Tarniceriu, P. Renevey, M. Bertschi, R. Delgado-Gonzalo and I. Korhonen, "Evaluation of the beat-to-beat detection accuracy of PulseOn wearable optical heart rate monitor," *37th Annual International Conference of the IEEE Engineering in Medicine and Biology Society (EMBC,* pp. 8099-8102, 2015.

[91] A. Tarniceriu, J. Harju, A. Vehkaoja, J. Parak, R. Delgado-Gonzalo, P. Renevey, A. Yli-Hankala and I. Korhonen, "Detection of beat-to-beat intervals from wrist photoplethysmography in patients with sinus rhythm and atrial fibrillation after surgery," in *2018 IEEE EMBS International Conference on Biomedical & Health Informatics (BHI)*, 2018.

APPENDIX A

In Table 5, the numeric values of HRV parameters error estimation without applying ectopic beat removal methods are provided.

Table 5. *The result of HRV metrics error estimation without applying any ectopic beat removal methods.*

Parameters		MAE	MAE (%)	RMSE	RMSE (%)	P05	P95	Bias	Bias (%)	SD
SDNN	[ms]	7.11	20.20	11.41	36.24	-17.13	19.40	0.47	9.95	13.68
RMSSD	[ms]	12.58	62.21	18.81	101.75	-23.29	34.73	4.08	52.25	23.17
pNN50	[%]	2.19	132.56	3.17	257.46	-3.13	6.5	0.99	98.23	3.60
NN50	[beats]	7.25	195.57	10.41	352.07	-17.0	18.0	1.51	167.47	12.71
IQR	[ms]	4.37	10.07	7.47	14.48	-10.5	7.25	-0.25	2.49	9.28
Median	[ms]	4.24	0.47	5.04	0.56	-6.0	8.0	0.27	0.03	5.42
Mean RR	[ms]	5.06	0.56	6.39	0.71	-7.56	11.16	0.46	0.05	6.93
Kurtosis	[-]	15.29	276.48	34.11	758.14	-20.50	68.48	6.33	259.78	38.28
Variance	[ms]	832.22	57.41	1468.2	143.19	-2123	1779.83	-124.95	39.65	2282.10
Mode	[ms]	14.94	1.64	22.54	2.53	-33.0	29.0	-1.91	-0.15	28.79
HR Mean	[BPM]	0.38	0.56	0.48	0.70	-0.85	0.54	-0.03	-0.05	0.51
TRI	[-]	0.88	11.76	1.16	15.12	-2.0	1.87	0.07	3.59	1.22
TINN	[ms]	0.01	11.83	0.01	17.18	-0.03	0.02	0.001	4.37	0.01
VLF Abs	[ms^2]	478.16	30.87	688.17	46.87	-1644.62	332.02	-367.20	-12.90	626.72
LF Abs	[ms^2]	178.67	35.95	261.64	60.75	-439.17	450	21.17	17.2	269.48
HF Abs	[ms^2]	252.16	78.80	350.34	131.20	-553.92	676.15	91.56	64.98	358.28
LF Norm	[n.u.]	10.08	25.75	13.67	39.42	-33.29	16.83	-4.31	3.35	14.52
HF Norm	[n.u.]	10.08	41.18	13.67	63.04	-16.83	33.29	4.31	31.93	14.52
VLF Log	[log]	0.38	5.50	0.57	8.17	-1.27	0.39	-0.26	-3.39	0.53
LF Log	[log]	0.29	4.98	0.42	7.19	-0.68	0.79	0.05	1.22	0.44
HF Log	[log]	0.44	8.12	0.58	11.21	-0.56	1.53	0.25	5.41	0.62
VLF Rel	[%]	10.59	23.78	14.94	36.85	-33.66	9.21	-7.70	-8.46	13.70
LF Rel	[%]	4.89	34.44	7.11	60.47	-6.52	15.44	2.69	26.44	6.83
HF Rel	[%]	9.05	106.52	12.79	183.55	-14.47	28.42	5	97.06	12.68
LF/HF	[n.u.]	1.01	48.96	1.48	79.05	-4.85	0.59	-0.75	5.34	2.20
ApEn	[-]	0.09	11.04	0.12	17.43	-0.11	0.28	0.04	6.94	0.12
SD_1	[ms]	8.90	62.22	13.30	101.76	-16.47	24.56	2.88	52.25	16.38
SD_2	[ms]	7.07	15.75	11.98	28.73	-19.94	19.92	-0.02	5.69	13.37
SD_1/SD_2	[-]	0.15	47.13	0.20	67.21	-0.26	0.44	0.07	38.93	0.20
DFA α_1	[-]	0.18	10.52	0.24	13.91	-0.26	0.58	0.09	6.54	0.25
DFA α_2	[-]	0.12	6.57	0.18	9.77	-0.16	0.39	0.07	4.17	0.17